

Mechanisms for Formation of Super El Ninos

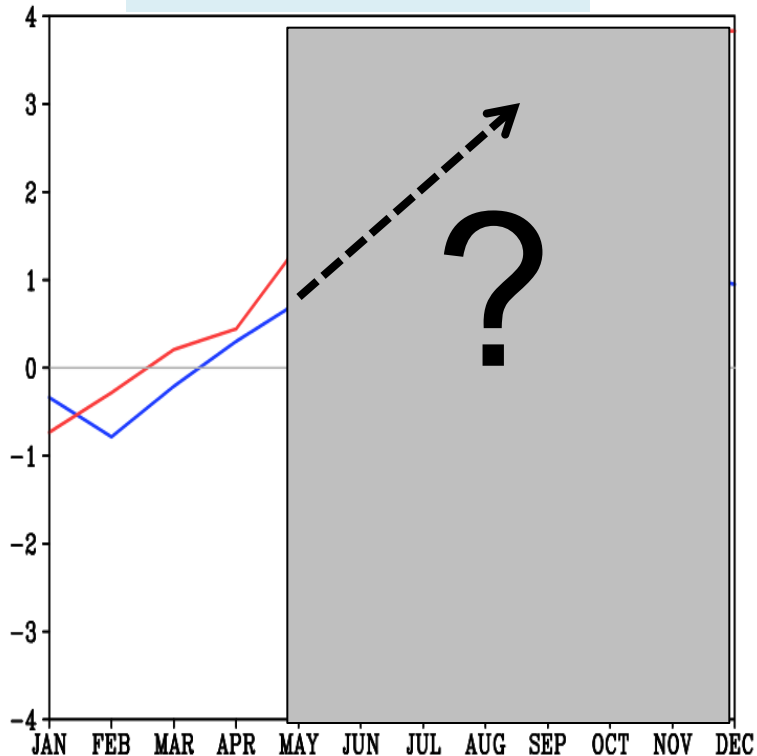
Tim Li

University of Hawaii at Manoa

Operational challenge: ENSO amplitude forecast

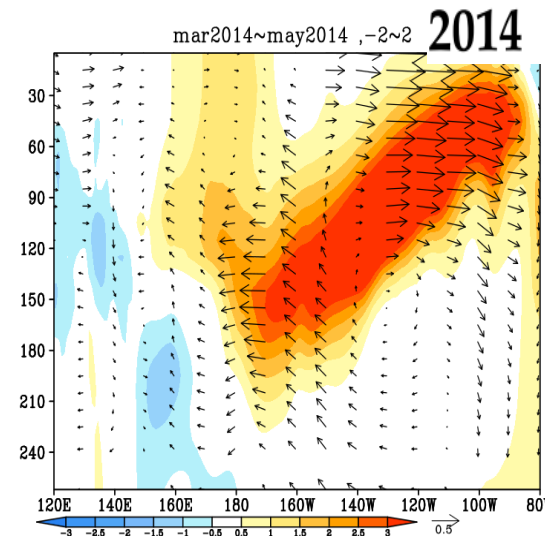
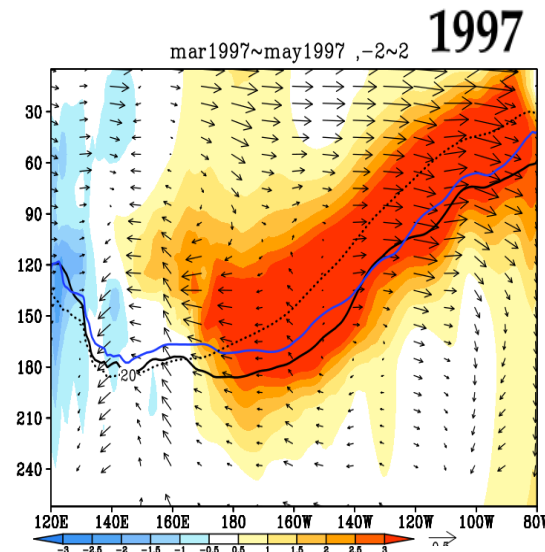
Examples: 2014 and 2015 El Niño events

Nino3 SSTA index



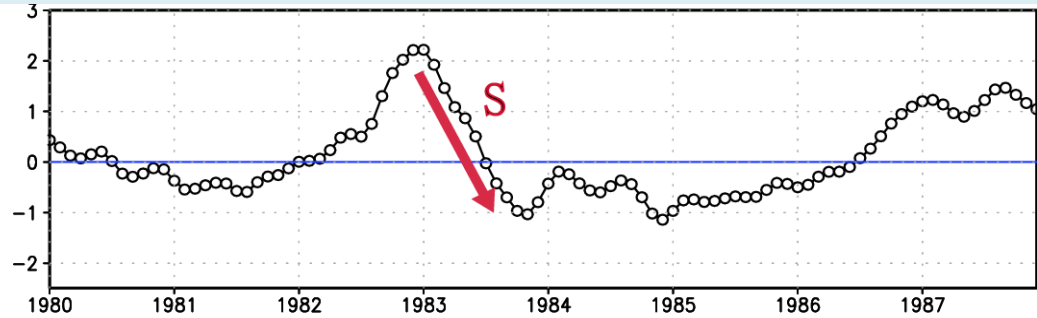
— 1997 SSTA

— 2014 SSTA

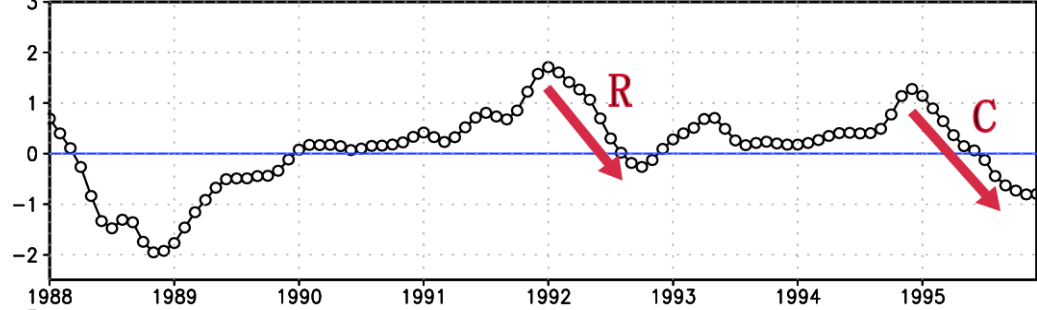


Similar oceanic and atmospheric preconditions in early 2014 and early 1997 led to speculation that a super El Niño was on the way (Tollefson 2014, *Nature*). But this was not materialized.

An El Nino is typically followed by a cold SSTA in EEP, but after a weak 2014 El Nino, a super El Nino occurred in late 2015.

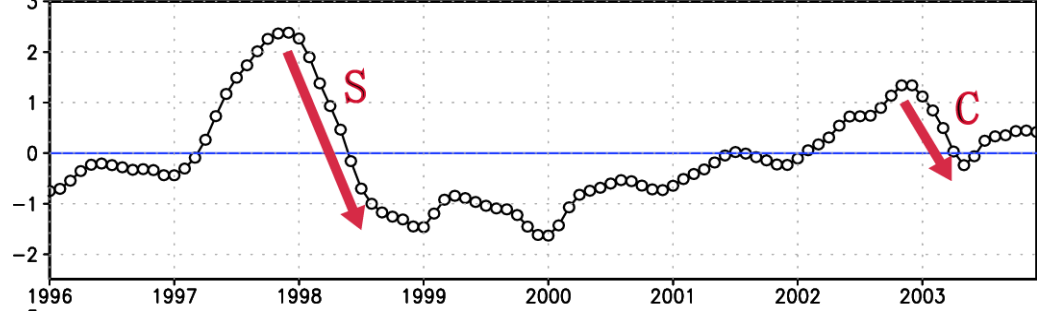


← Time series of Niño 3.4 SSTA from 1980 to 2011

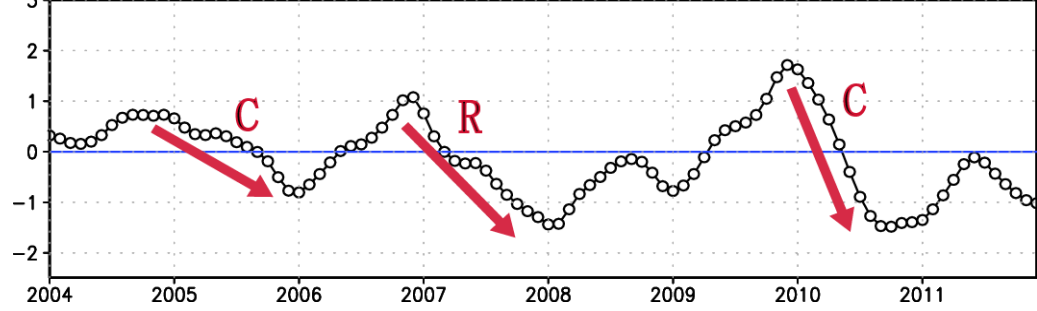


Super El Niño
(denoted by "S")

Regular El Niño
(denoted by "R")



CP El Niño
(denoted by "C")



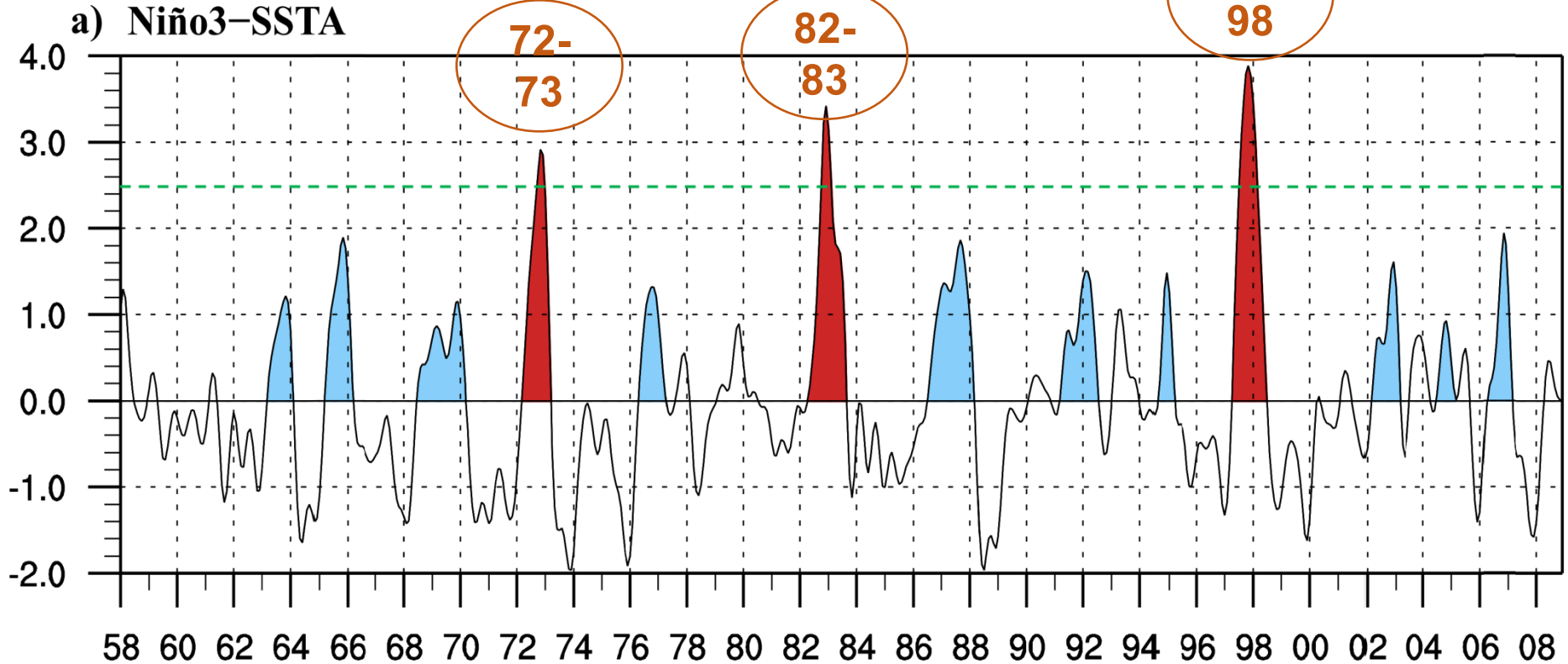
Chen, Li, et al. 2016, JC

Science Questions:

- What are fundamental differences of **precursory signals** between regular and super El Ninos?
- Is the **formation of 2015 super El Nino** different from previous super El Ninos in 1997 and 1982?

Precursory Difference between Super & Regular El Niño Events

Chen, Li et al. 2016, AAS

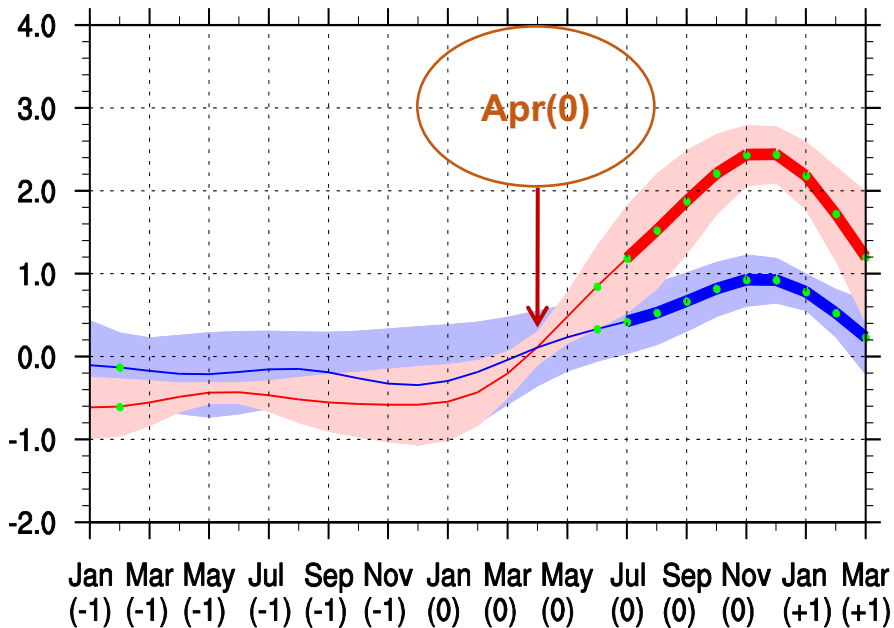


3 **super** El Niño events: 72-73, 82-83, 97-98 → **S-group**

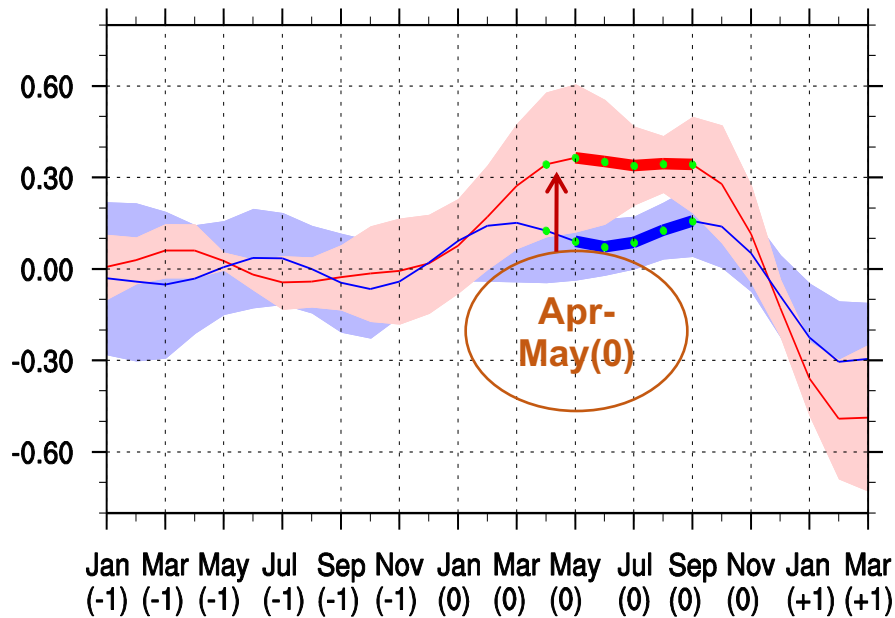
11 **Regular** El Niño events: 63-64, 65-66, 69-70, 76-77, 86-87, 87-88, 91-92, 94/95, 02/03, 04/05, 06/07 → **R-group**

Composite SSTA and SSTA-tendency in S-group and R-group

a) Temporal evolution of SSTA



b) Evolution of SSTA tendency

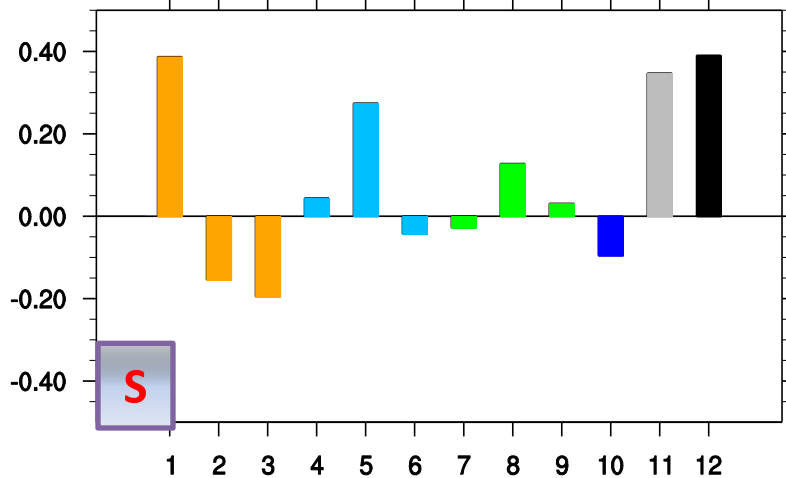


Positive **SSTA** starts at the same period (around Apr[0]) in both groups, but the **SSTA-tendency** of S-group during Apr-May[0] is three times as much as that in M-group.

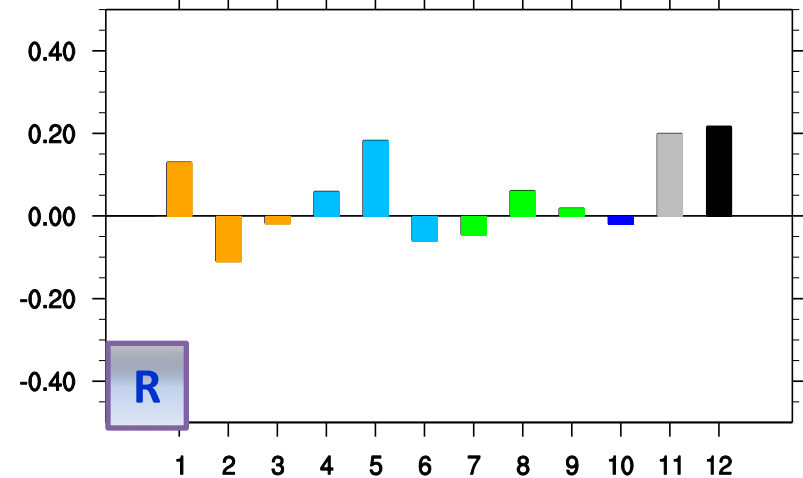
Such a significantly difference in the SSTA-tendency in the **onset stage (AM[0])** causes the divergent intensity in the following months.

ML heat budget results for **Onset Stage (AM[0])**

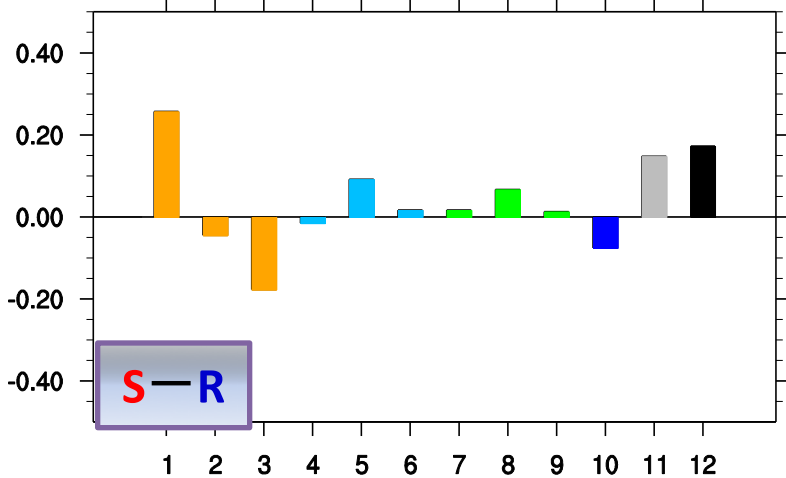
a) S-group




b) R-group



c) Diff (S minus R)

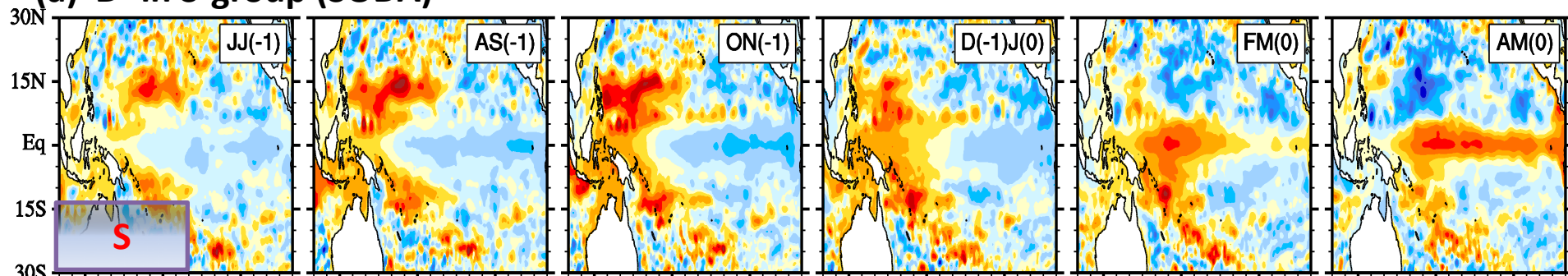


 Main difference in **Apr-May[0]** between the two groups lies in **zonal advective feedback** ($-u' \partial \bar{T} / \partial x$), and such a difference is attributed to zonal geostrophic current anomaly difference between S-group and R-group during initial developing stage.

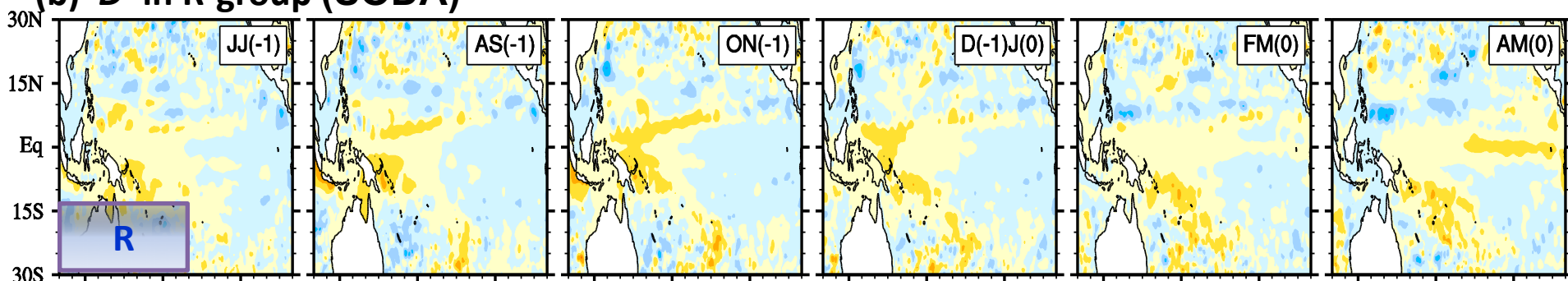
- (1) $-u' \partial \bar{T} / \partial x$ (2) $-\bar{u} \partial T' / \partial x$ (3) $-u' \partial T' / \partial x$ (4) $-w' \partial \bar{T} / \partial z$ (5) $-\bar{w} \partial T' / \partial z$ (6) $-w' \partial T' / \partial z$
 (7) $-v' \partial \bar{T} / \partial y$ (8) $-\bar{v} \partial T' / \partial y$ (9) $-v' \partial T' / \partial y$ (10) $Q' / \rho C_p H$ (11) Adv+Qnet (12) $\partial T' / \partial t$

D' in Pre-onset stage (Chen, Li et al. 2016, AAS)

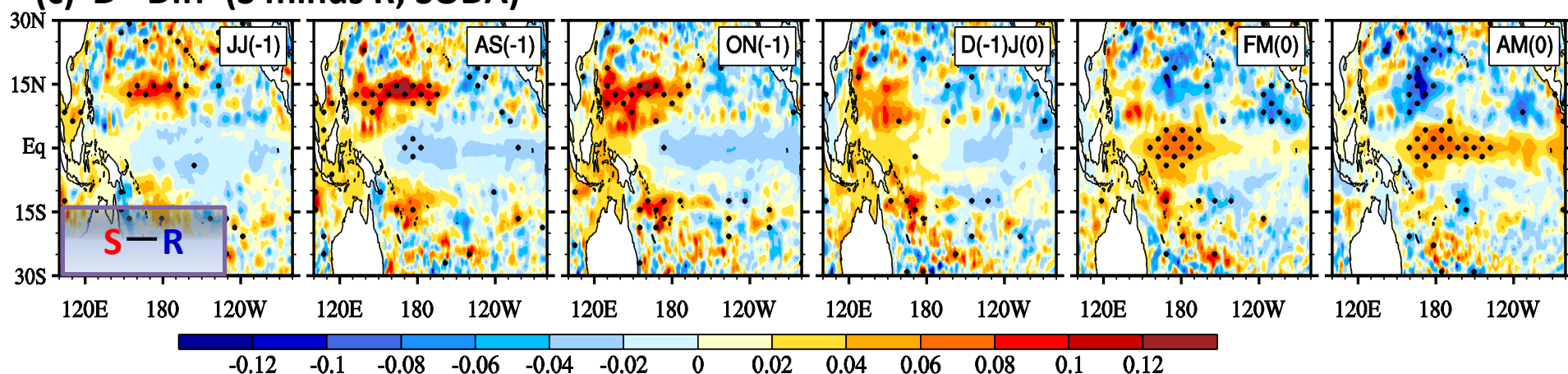
(a) D' in S-group (SODA)



(b) D' in R-group (SODA)



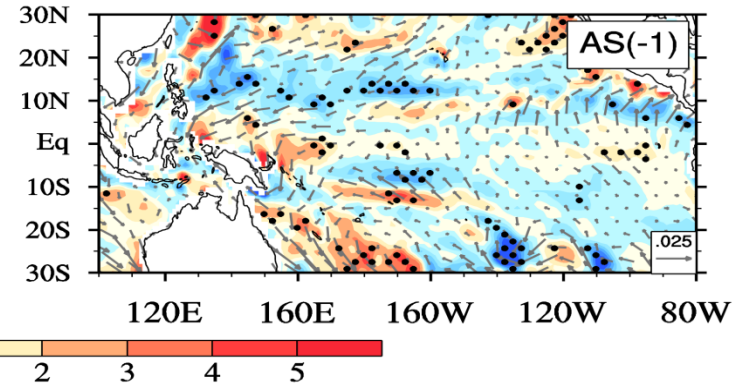
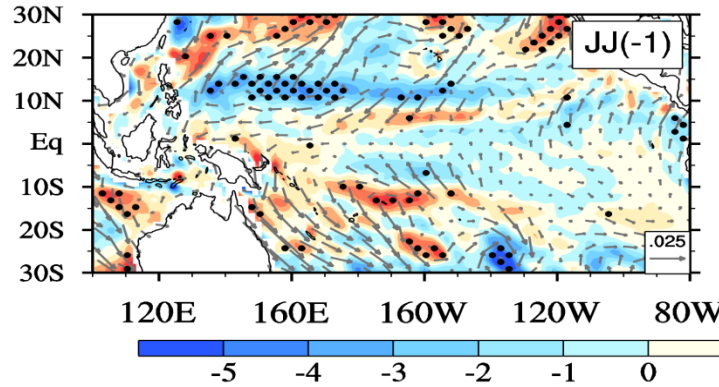
(c) D' Diff (S minus R; SODA)



Distinctive **Wind Stress Curl'**, **Precipitation'** and **SST'** in JJAS[-1] between S and R group

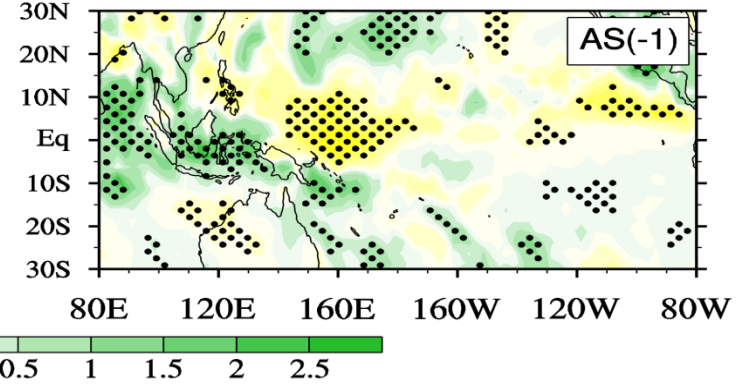
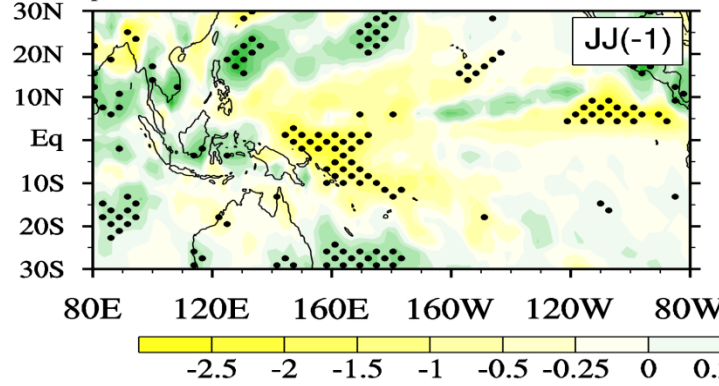
Diff_Wind stress C_{url}' (shading; units: 10^{-8} N m^{-3})

(a) Wind stress C_{url}' Diff (S minus R)



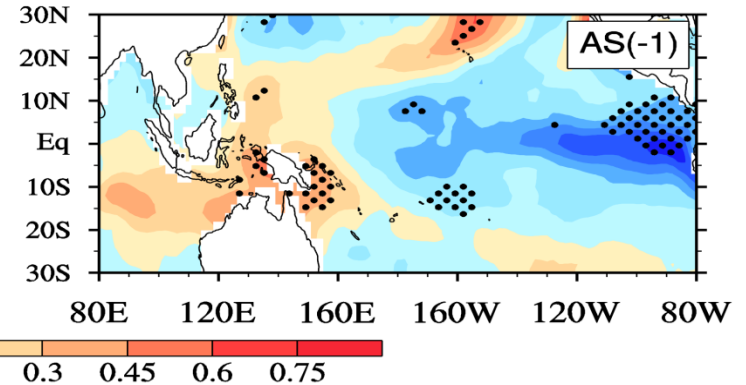
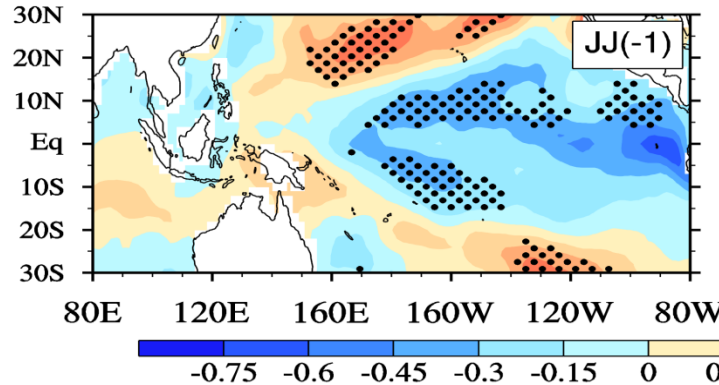
Diff_ P_r'

(b) P_r' Diff (S minus R)



Diff_ SST'

(c) $SSTA$ Diff (S minus R)



Summary

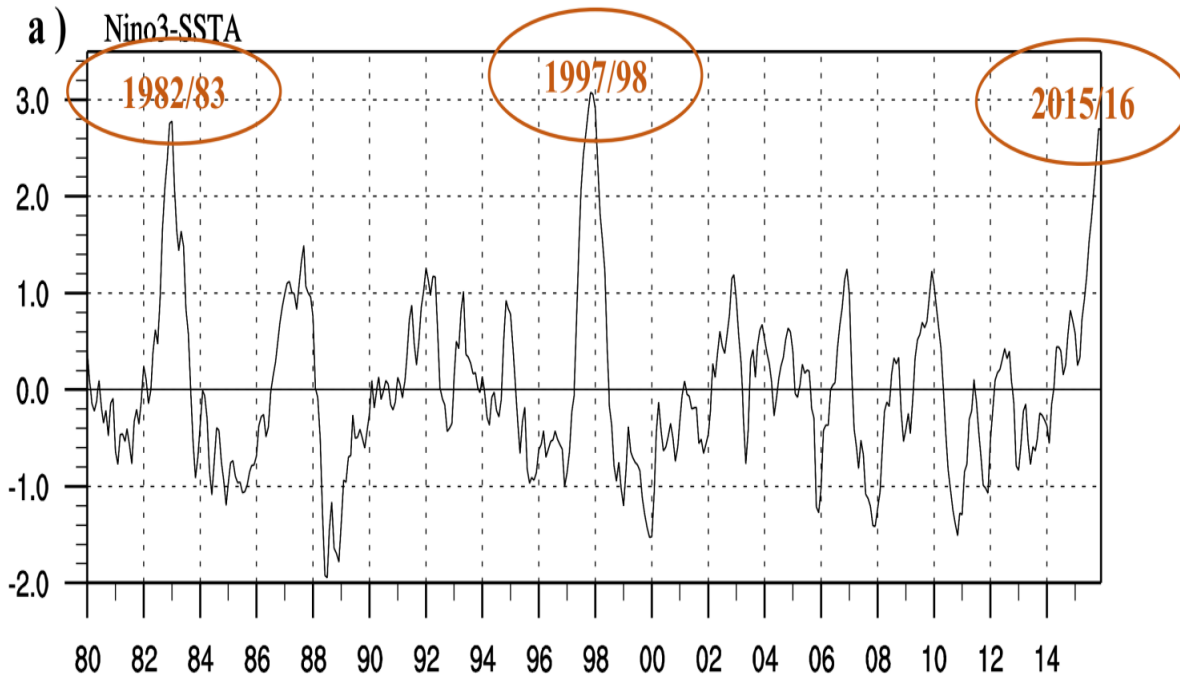
✚ Statistically significant difference between super and regular El Niño group lies in the **SSTA-tendency** difference during Apr-May[0]: SSTA tendency is much greater in S-group than M-group.

✚ The cause of the SSTA tendency difference lies in the **zonal advective feedback**, as u' is stronger in S-group than M-group in the initial developing stage.

✚ The difference in u' is caused by the difference in the **anomalous thermocline depth (D')**, which is associated **with the difference in the** anomalous wind, precipitation and SST pattern prior to the El Niño onset.

Formation Mechanism of 2015 Super El Niño

Tim Li, Lin Chen, and Bin Wang
University of Hawaii



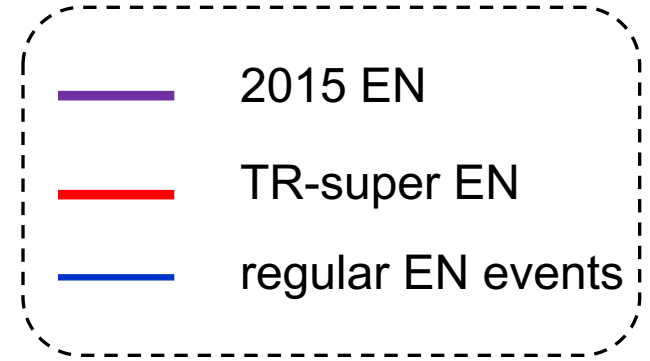
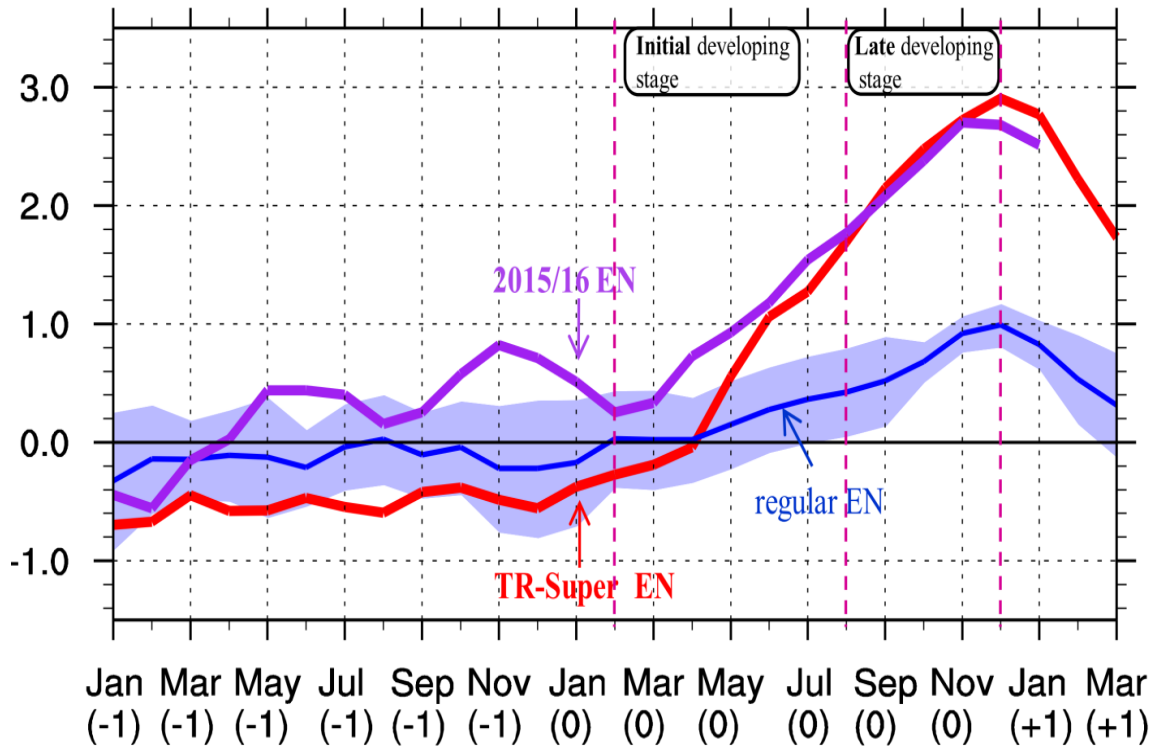
Science Questions:

How did the 2015 El Niño form?

Was the development of 2015 El Niño similar to that of traditional super El Niño in 1982/83 and 1997/98?

Chen, L., T. Li, B. Wang, 2017: Formation Mechanism for 2015/16 Super El Niño. *Scientific Reports*, 7 (2975), doi:[10.1038/s41598-017-02926-3](https://doi.org/10.1038/s41598-017-02926-3).

2015 Super El Nino vs. 1997/1982 Super El Nino: Two Distinctive Routes



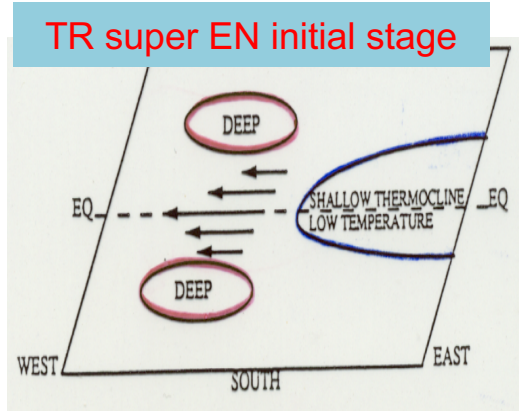
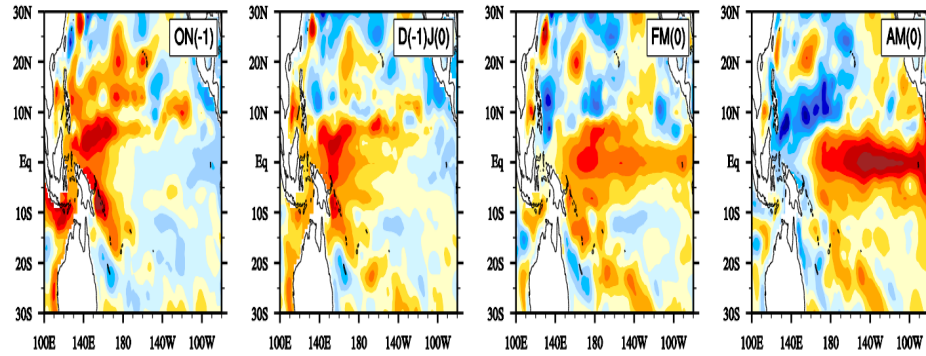
Initial developing stage (Feb-Jul)

Late developing stage (Aug-Nov)

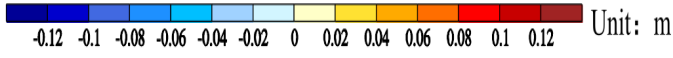
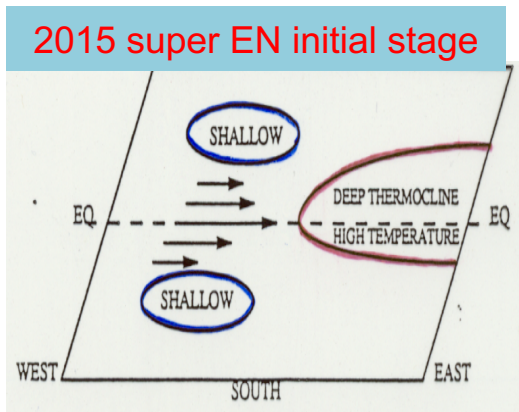
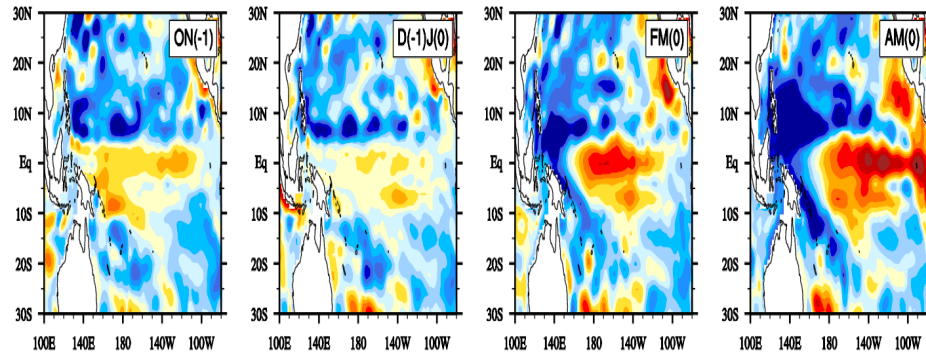
- (1) **TR-super EN** started from **a cold episode**, while **2015 EN** started from **a weak warming** in EP in the preceding year;
- (2) For 2015 EN, a **marked turnabout** of the SSTA tendency (from negative to positive) happened around **February 2015**.

Precursory D' Evolution during Initial Onset Stage

(a) D' (TR-super EN)



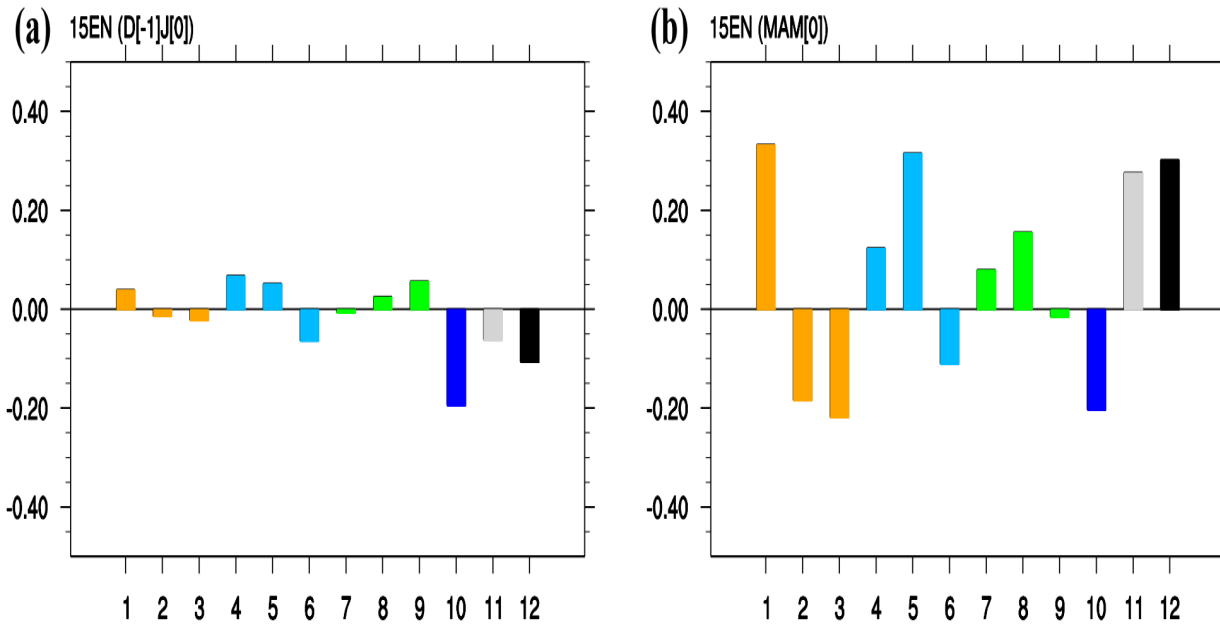
(b) D' (2015 EN)



- ✓ **Traditional view of El Nino formation dynamics:** Piling-up of warmer water in off-equatorial western Pacific is a pre-conditioning for formation of an El Nino.
- ✓ Precursory D' in late 2014/early 2015 was **unfavorable** for an El Nino to occur, but a positive D' center **unexpectedly** appeared in CEP in FM[0] 2015.

Mixed-Layer Heat Budget Diagnosis:

Role of D' in sign change of SSTA tendency in Feb 2015



geostrophic current:

$$u_g = -\frac{g'}{\beta} \frac{\partial^2 h}{\partial y^2}$$

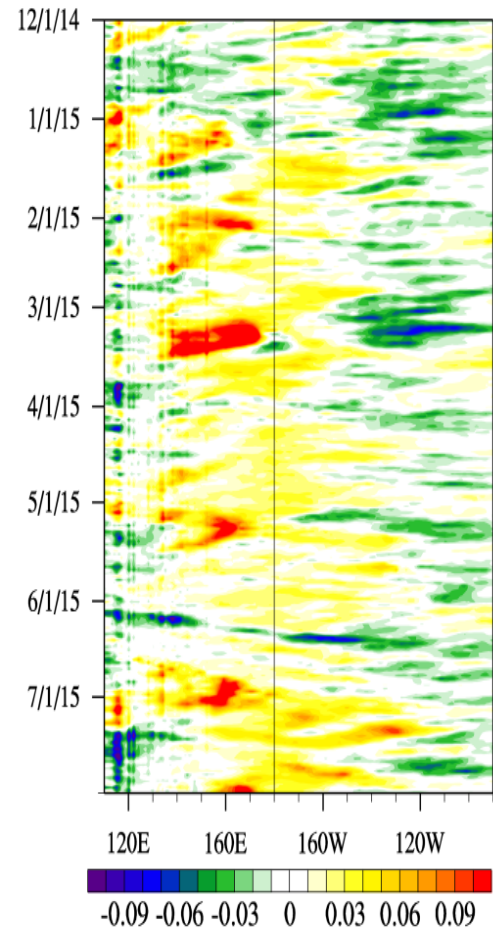
Mixed layer temperature tendency equation:

$$\begin{aligned} \partial T' / \partial t = & \underbrace{-u' \partial \bar{T} / \partial x}_{\text{term 1}} \underbrace{-\bar{u} \partial T' / \partial x}_{\text{term 2}} \underbrace{-u' \partial T' / \partial x}_{\text{term 3}} \underbrace{-w' \partial \bar{T} / \partial z}_{\text{term 4}} \underbrace{-\bar{w} \partial T' / \partial z}_{\text{term 5}} \underbrace{-w' \partial T' / \partial z}_{\text{term 6}} \\ & \underbrace{-v' \partial \bar{T} / \partial y}_{\text{term 7}} \underbrace{-\bar{v} \partial T' / \partial y}_{\text{term 8}} \underbrace{-v' \partial T' / \partial y}_{\text{term 9}} + \underbrace{\frac{Q'_{net}}{\rho C_p H}}_{\text{term 10}} + R \end{aligned}$$

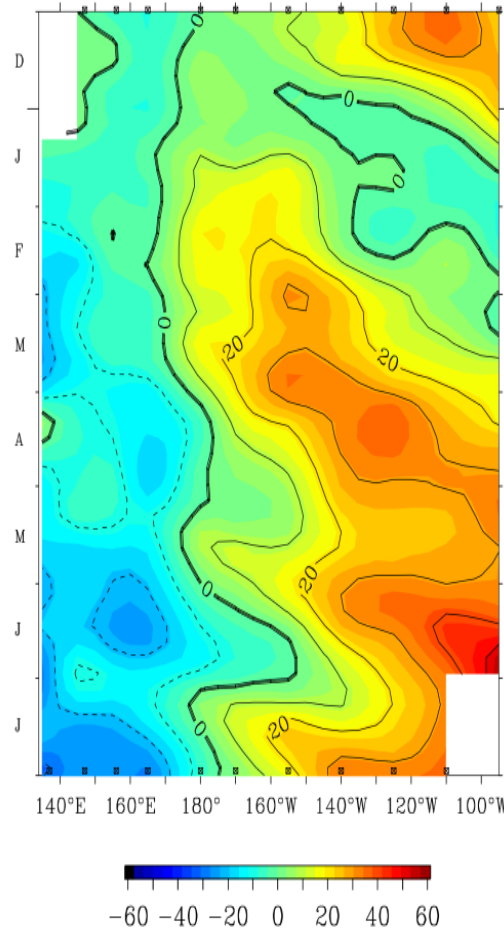
The warming in MAM[0] was primarily caused by **zonal advective feedback** (term 1) and **thermocline feedback** (term 5), both of which were **related to D'** .

What caused the sudden increase of D' over equatorial Pacific in early 2015 ?

(a) $Taux'$ (2014Dec – 2015Jul)



(c) TAO Z_{20} Anomaly



Previous studies suggested that **high-frequency (HF) zonal wind forcing** such as westerly wind events (WWE) is important for the development of El Niño.

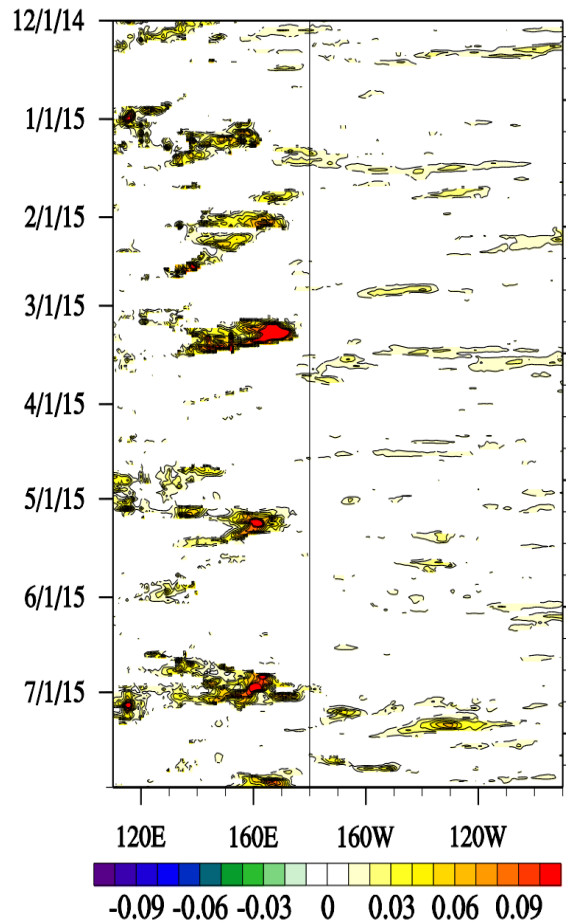
Note that there were a series of WWEs over equatorial Pacific during early 2015.

Did such events happen each year, or were they unusual?

→ How to quantitatively measure the WWEs strength?

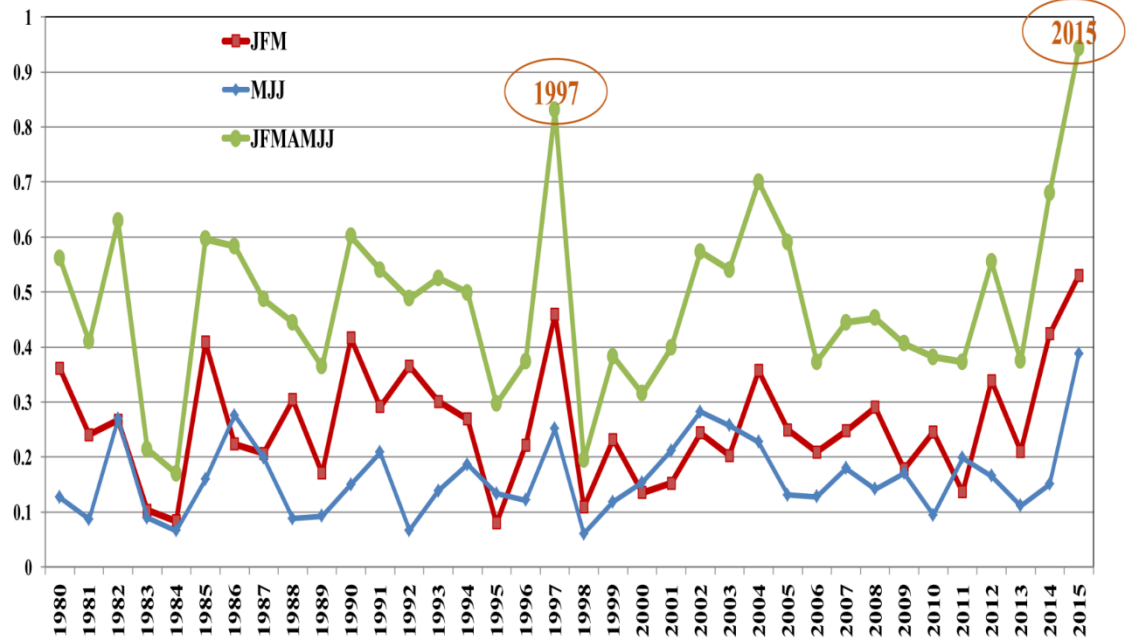
Accumulated WWE Index (AWI)

(b) *WWE-Taux'* (2014Dec – 2015Jul)



AWI is defined as **time integration of westerly wind stress anomalies** that exceed climatological standard deviation for a period of interest.

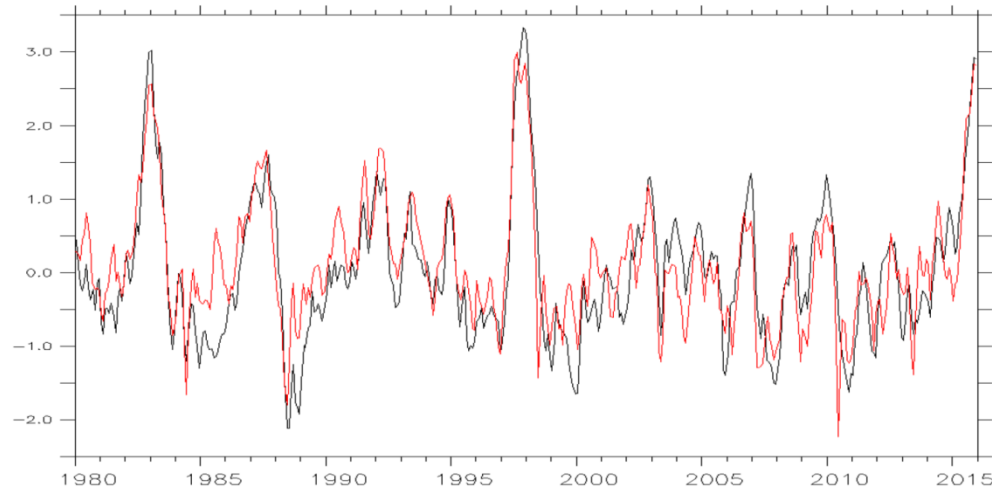
(d) Accumulated WWE-index (ensemble results from ERA-interim and NCEP2)



→ Our calculation indicates that the **strongest WWE events in the past 40 years (since 1979) happened in earlier 2015 !**

Role of HF Wind Forcing in Inducing D' -- OGCM (LICOM2.0) Experiments

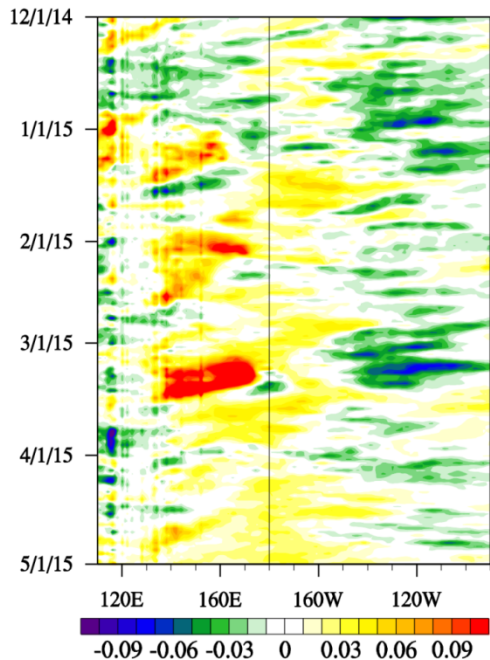
(a) Normalized Nino3-SSTA from ERSST (black) and CNTL-run (red)



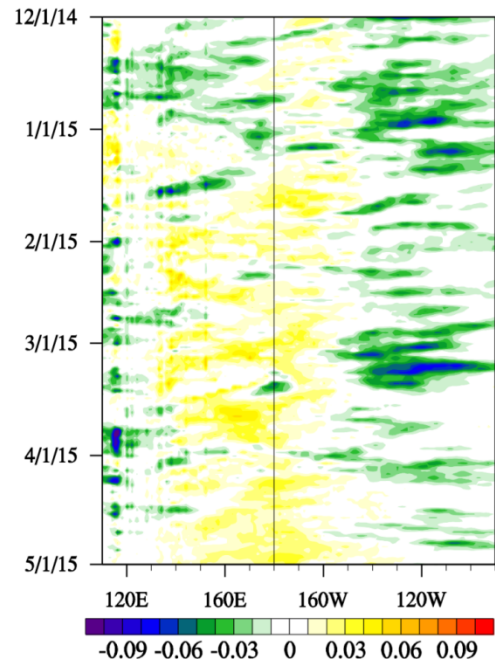
CNTL: Observed daily wind stress & heat flux forcing

No-WWE run: all forcing fields were kept the same as CNTL except that the HF WWE-Taux' component was removed.

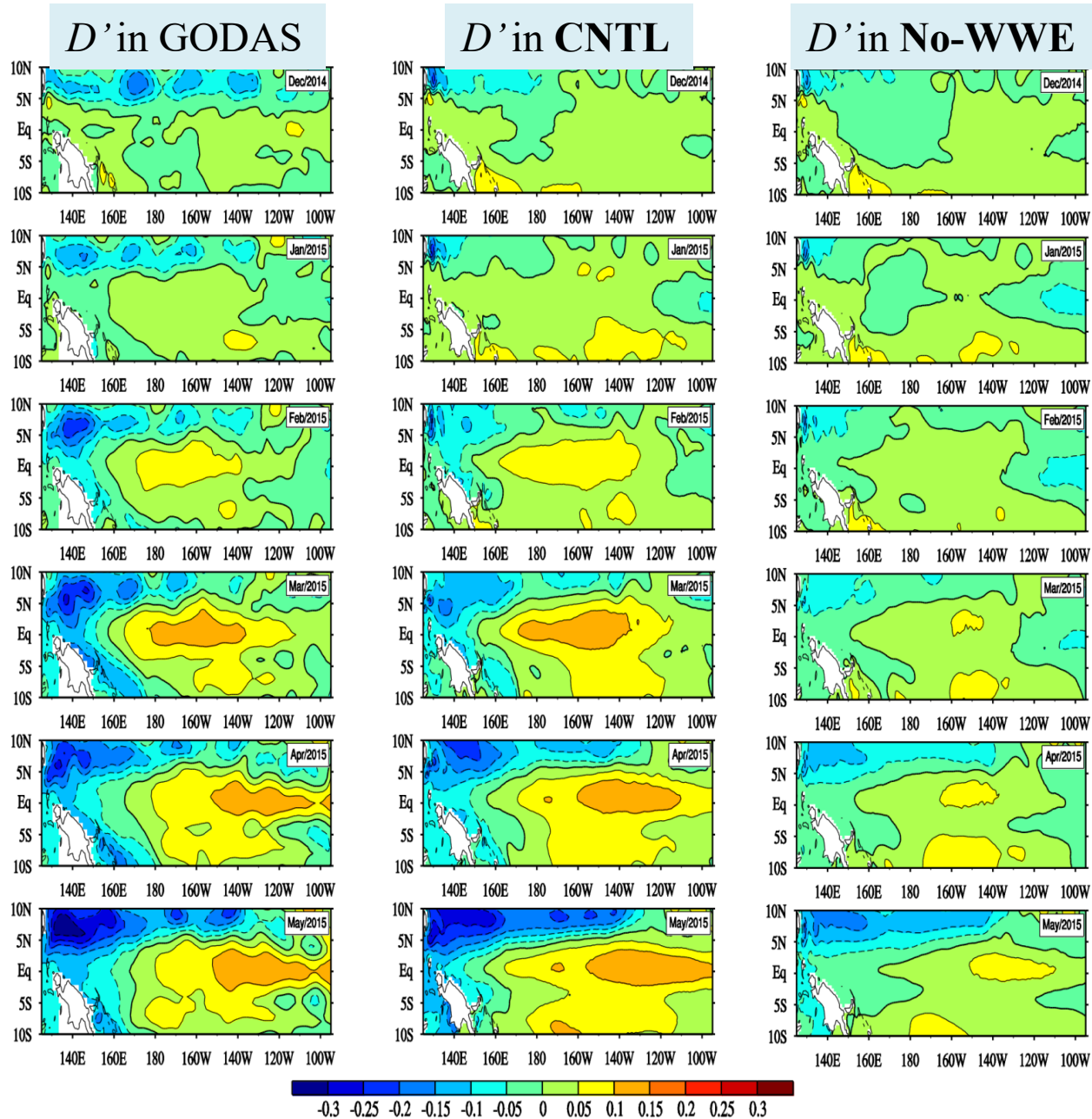
(b) $Taux'$ for CNTL



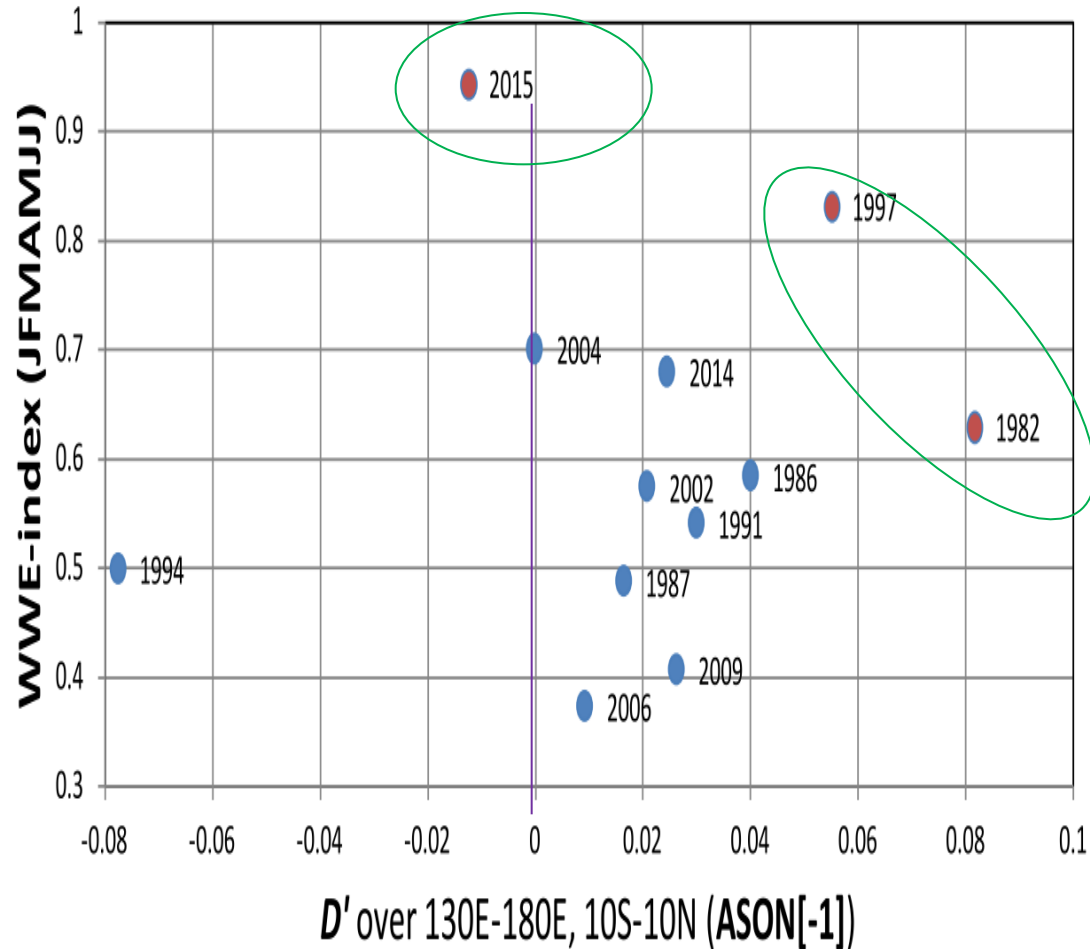
(c) $Taux'$ for No-WWE



Role of HF Wind Forcing in Setting-up D' -- OGCM Simulation Results



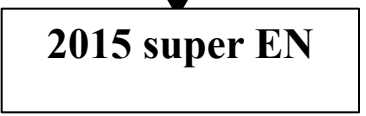
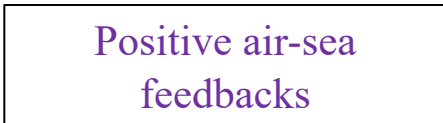
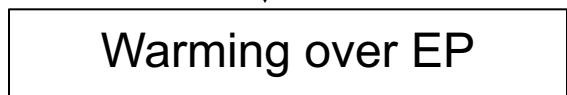
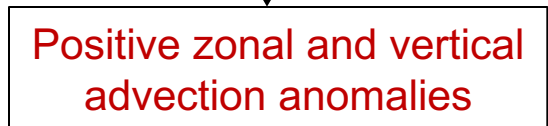
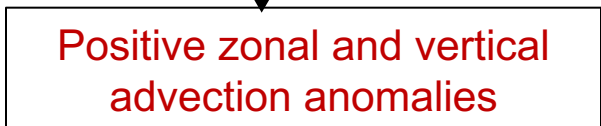
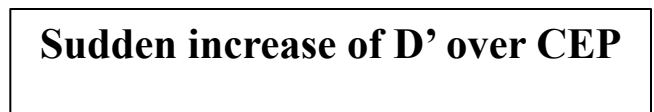
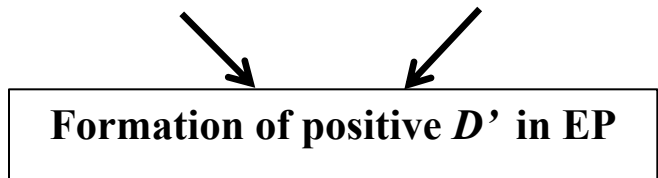
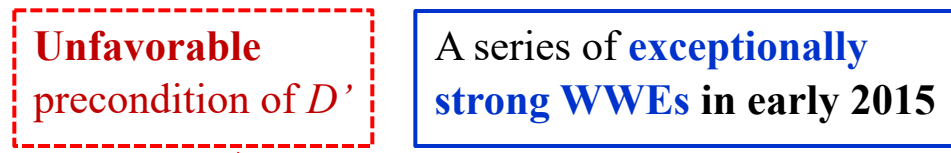
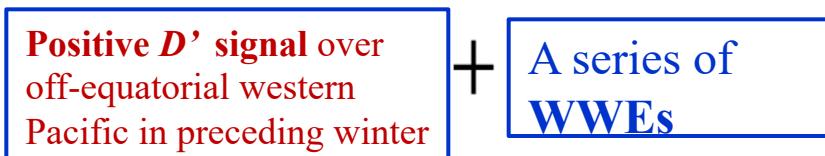
Two Distinctive Routes to Super El Nino Formation: Precursory D' vs. Accumulated WWE Index



Conclusion: Two super El Nino formation routes

Route I: Traditional super ENs

Route II: Special 2015 event



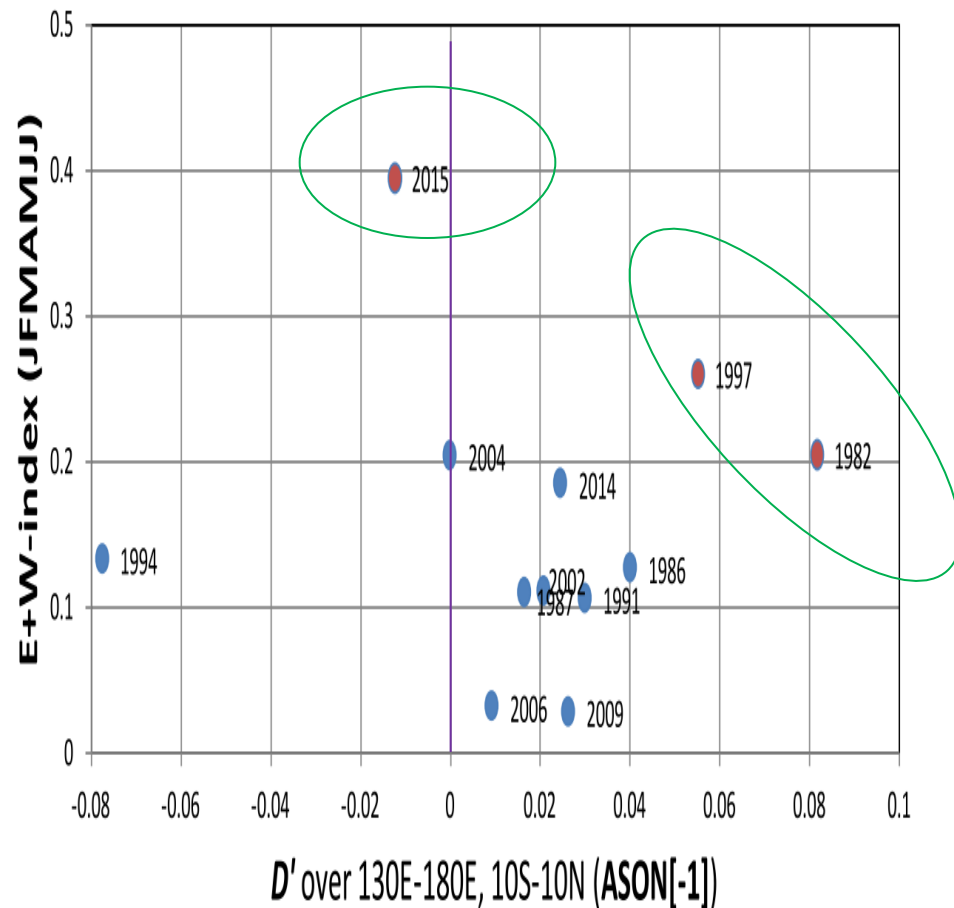
Thanks

Diamond Head



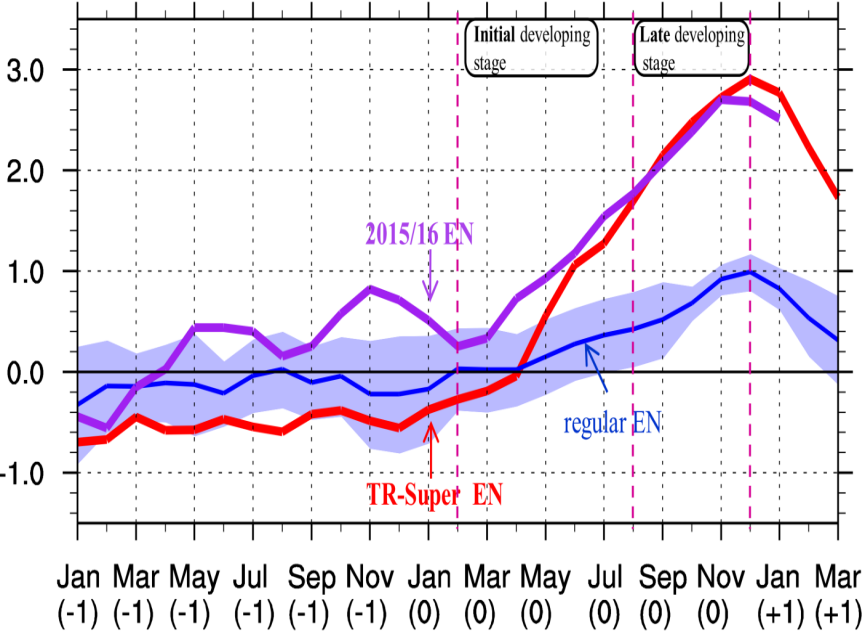
Two Distinctive Routes to Super El Nino Formation: Precursory D' vs. Combined WWEs/EWEs

(b) Conditions for each EN (D' v.s. "W+E" index)

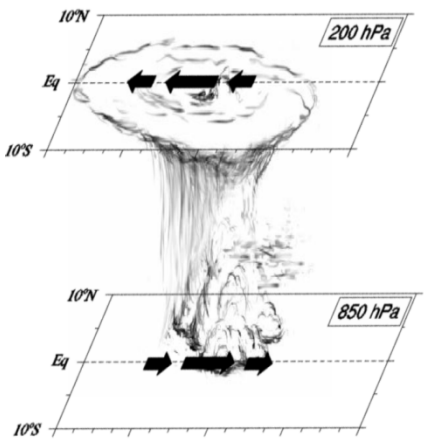


Growth Mechanism during Late Developing Stage -- Positive Atmosphere-Ocean Feedbacks

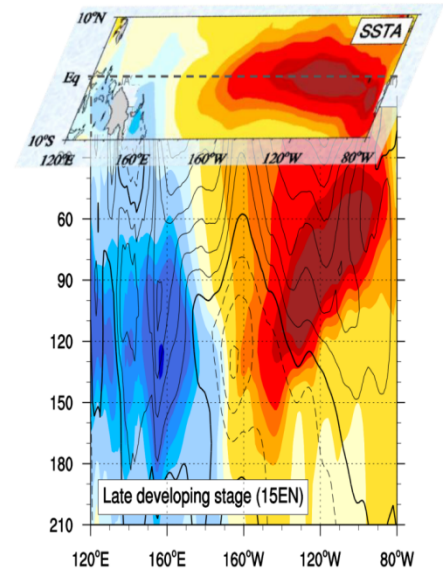
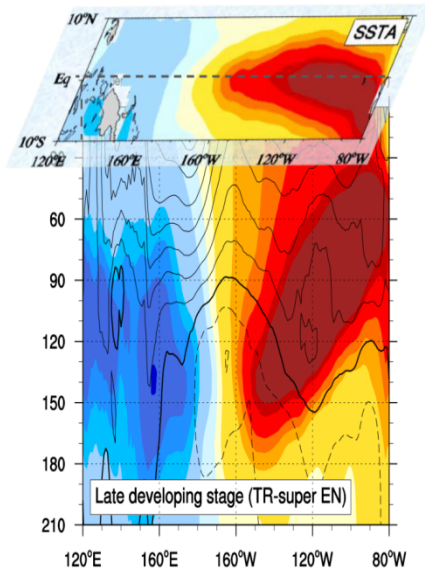
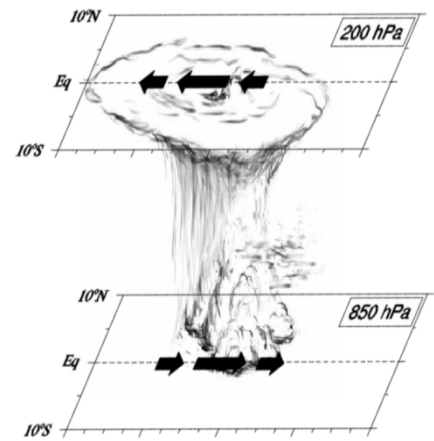
b) Time Evolution of SSTA



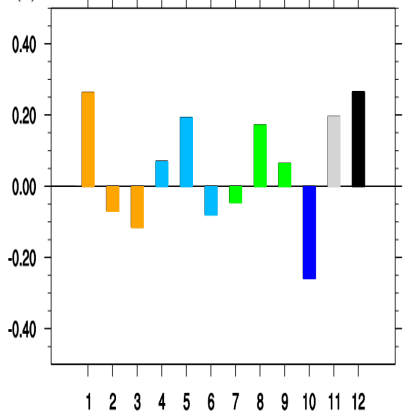
(a) TR-Super EN



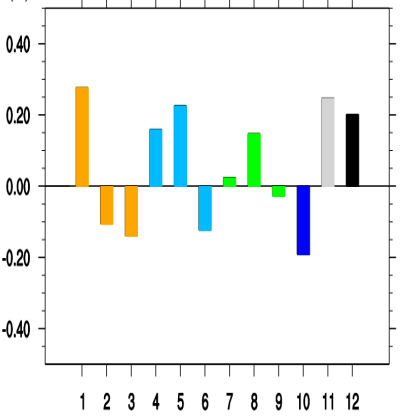
(b) 2015 EN



(a) TR-super EN (JASO[0])

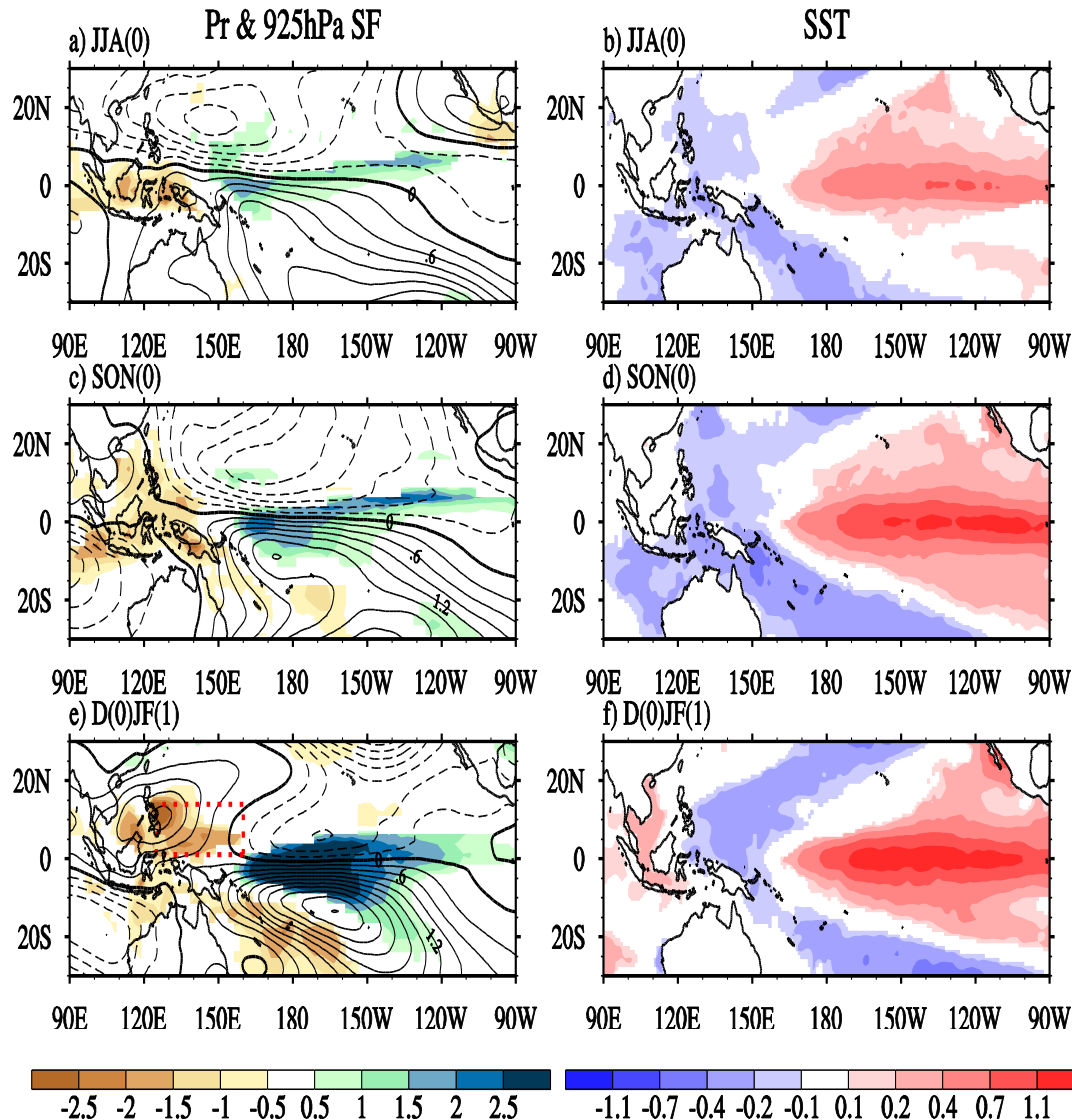


(b) 15-16 (JASO[0])



→ Theory 4: Moist enthalpy advection/Rossby wave modulation

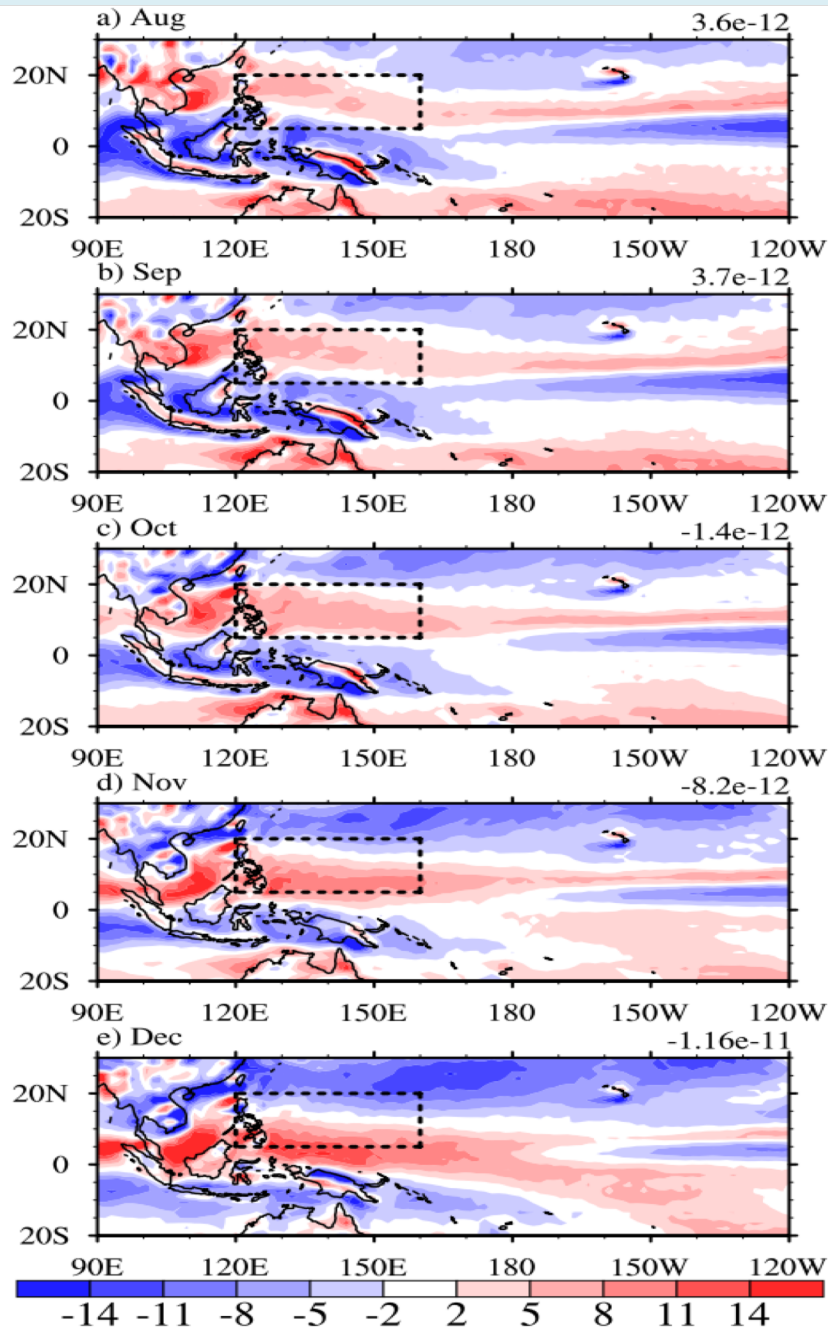
Wu, B, T. Zhou and Tim Li, Part 1 and Part 2, 2017, J. Climate



Left panels:
Precipitation
(shading, mm d^{-1})
and 925 hPa stream
function anomalies
(contours) regressed
against the DJF
Nino-3.4 index

Right panels:
Regressed SST
anomalies (K).

Background Meridional Vorticity Gradient Change

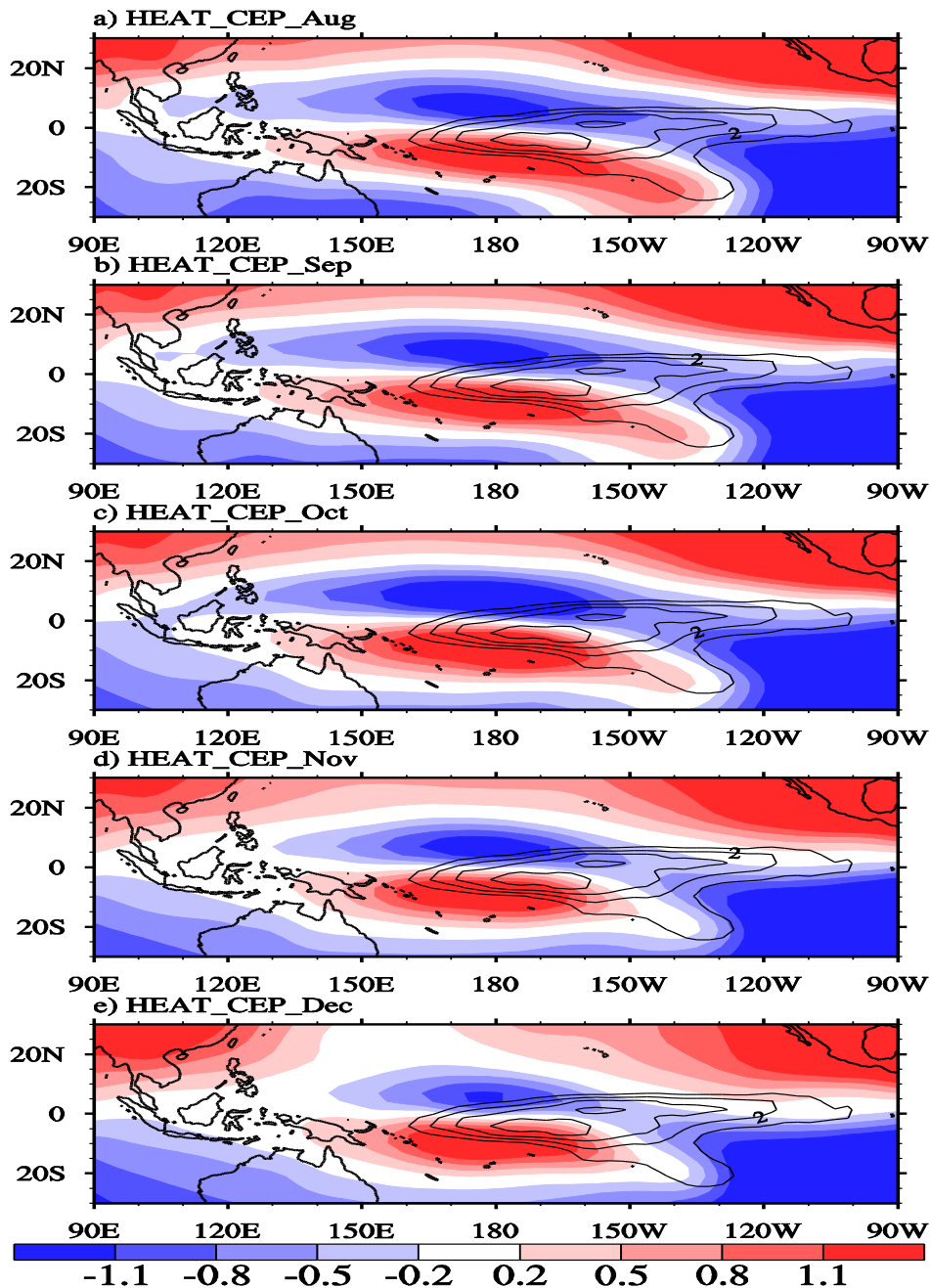


Shaded: Climatological mean **relative vorticity** field at 850hPa from August to December (from ERA-I)

Equivalent beta effect

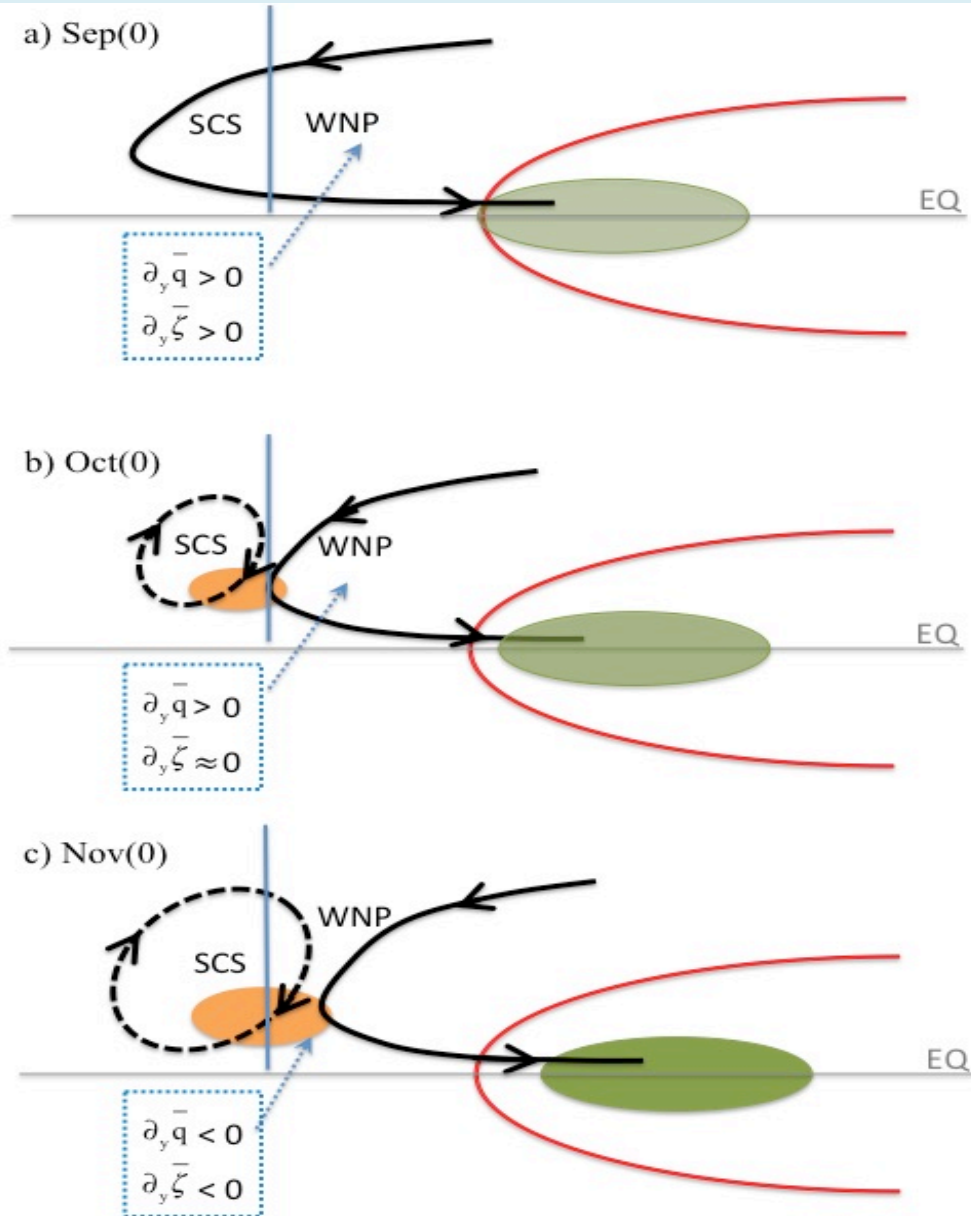
$$\beta_* = \beta + \partial_y \bar{\zeta}$$

Atmospheric Responses to a Specified El Niño-like Heating



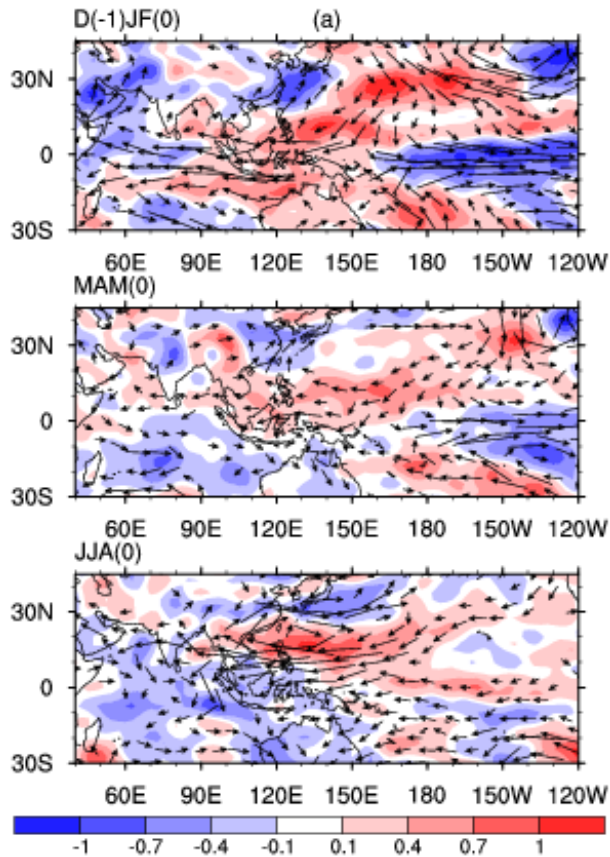
850hPa **stream function** anomalies (shading, 10^6 $\text{m}^2 \text{s}^{-1}$) simulated by an **anomaly AGCM** with a fixed heating structure

Schematic for WNPAC Formation – A Moist Enthalpy Advection – Rossby Wave Modulation Mechanism

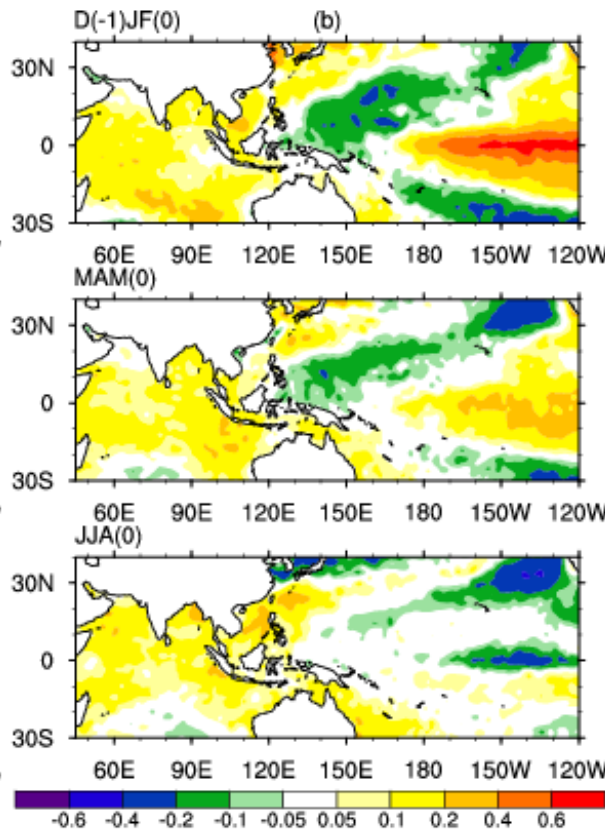


El Nino composite (1950-2006)

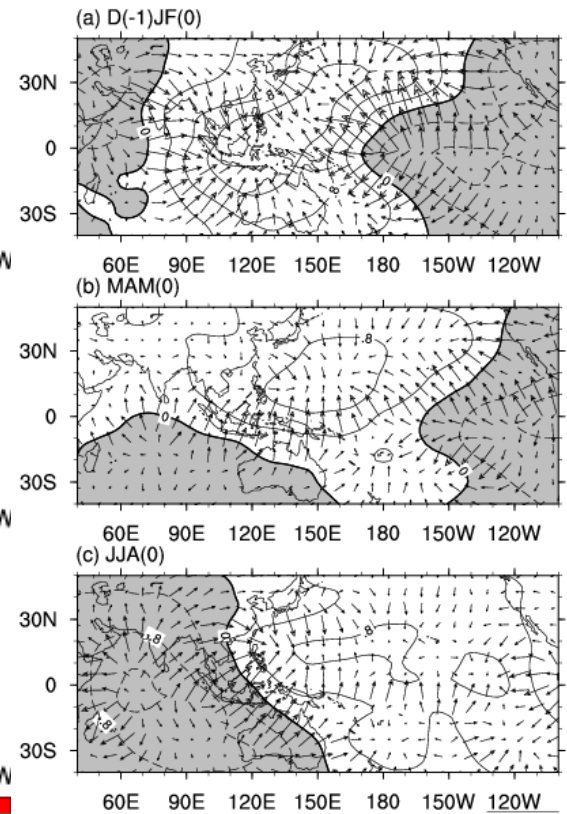
UV850, OMEGA500



SST



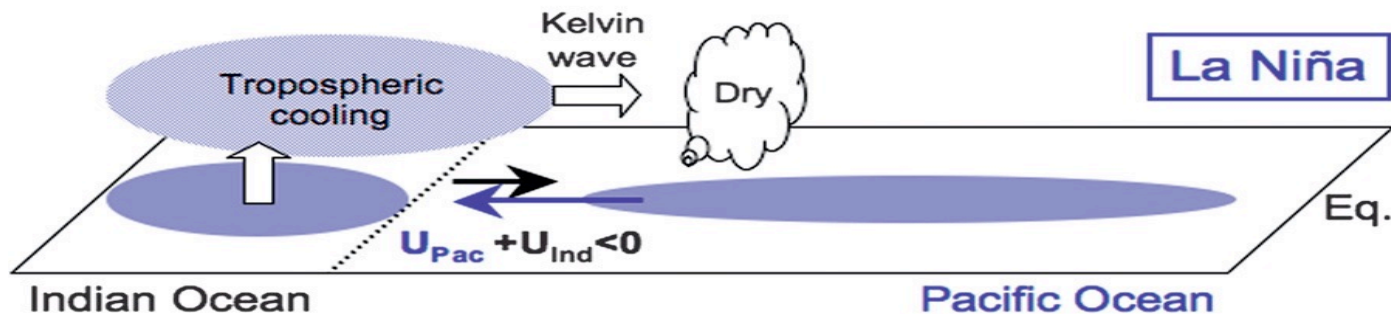
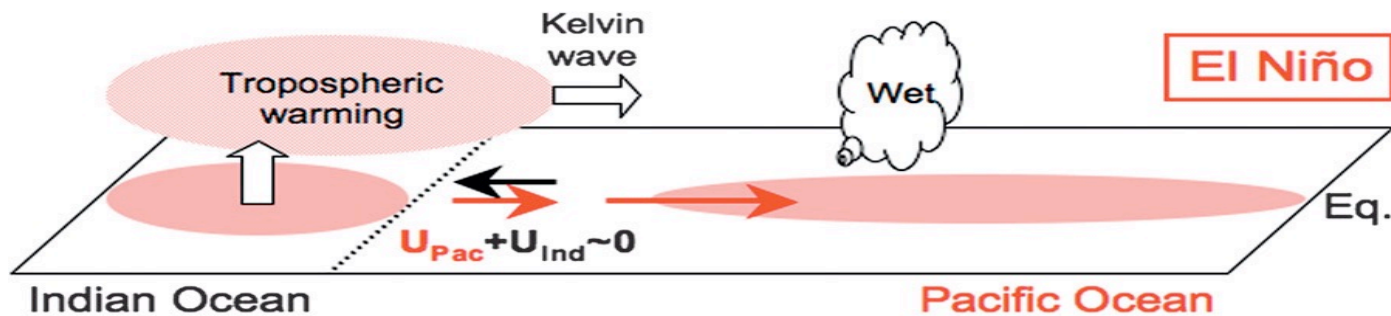
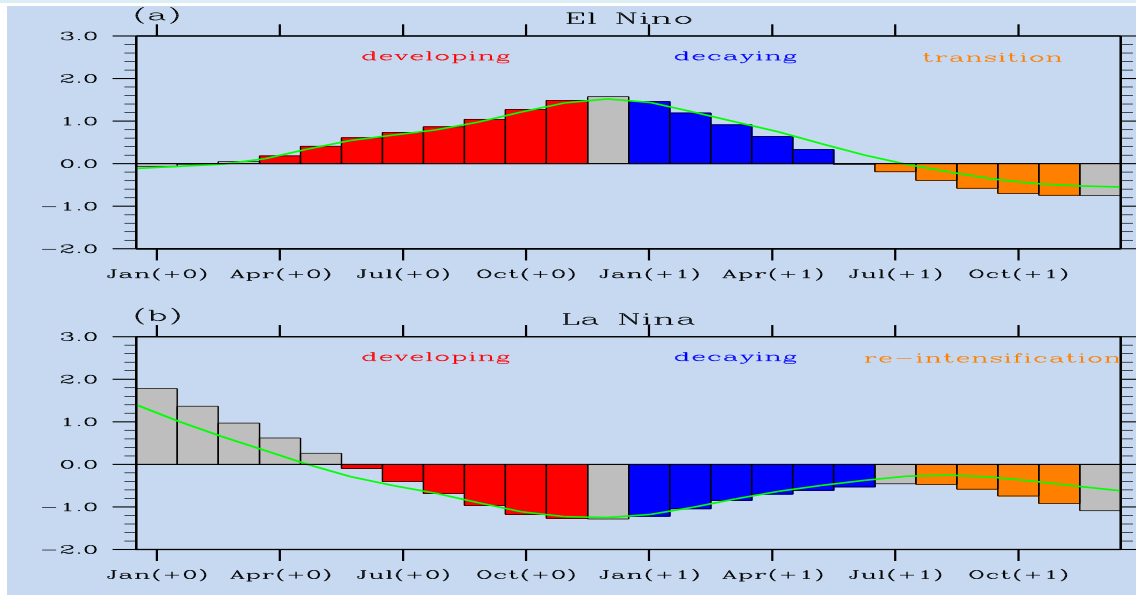
200hPa velocity potential



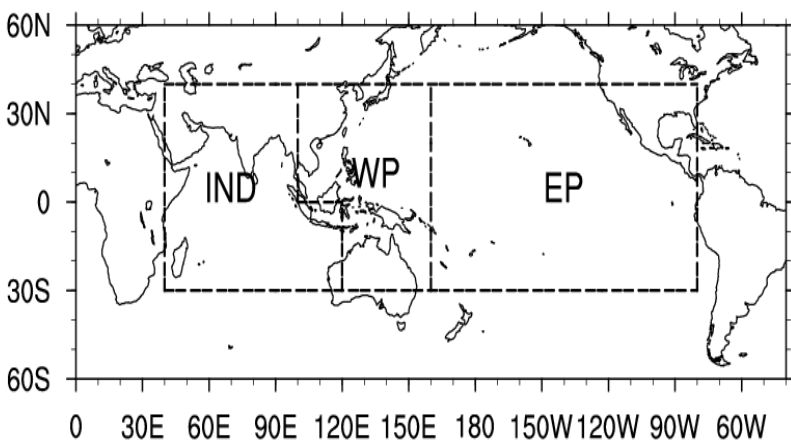
The IO capacitor effect becomes effective only during El Niño decaying summer!

→ A season-dependent IOBM forcing mechanism (Wu et al. 2009)

Evolution asymmetry mechanism: Wind vs. heat flux effect

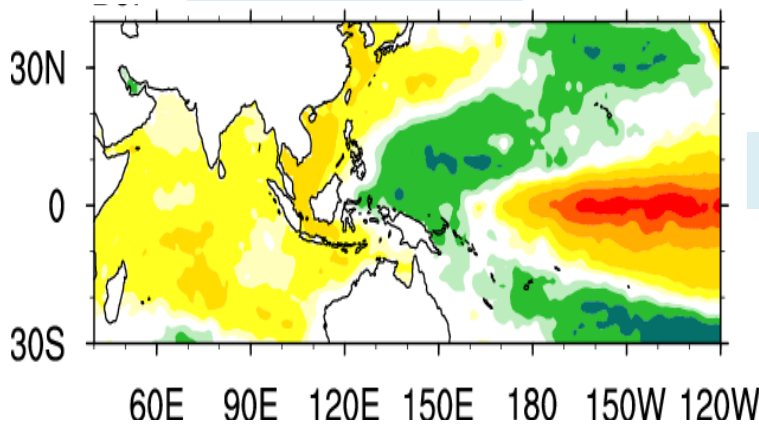


Okumura and
Deser 2010,
JC

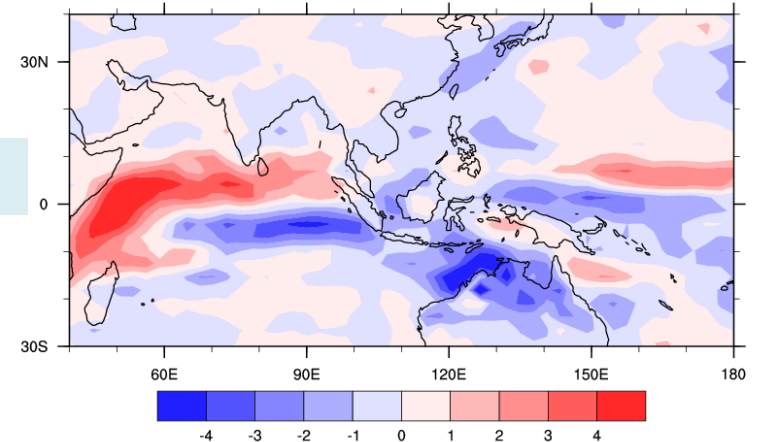


Mixed-layer heat budget analysis indicates that both anomalous wind stress and surface heat fluxes contribute to the ENSO evolution asymmetry!

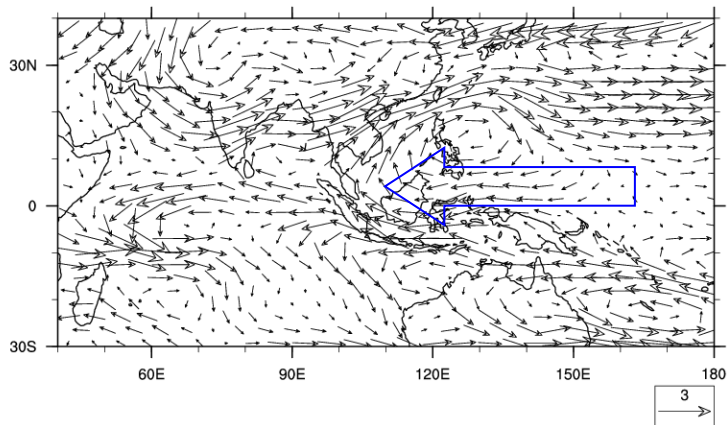
DJF SSTA



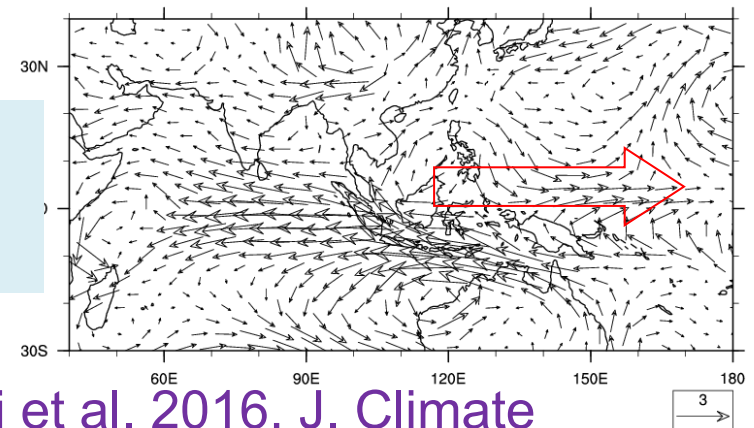
DJF precipitation anomaly



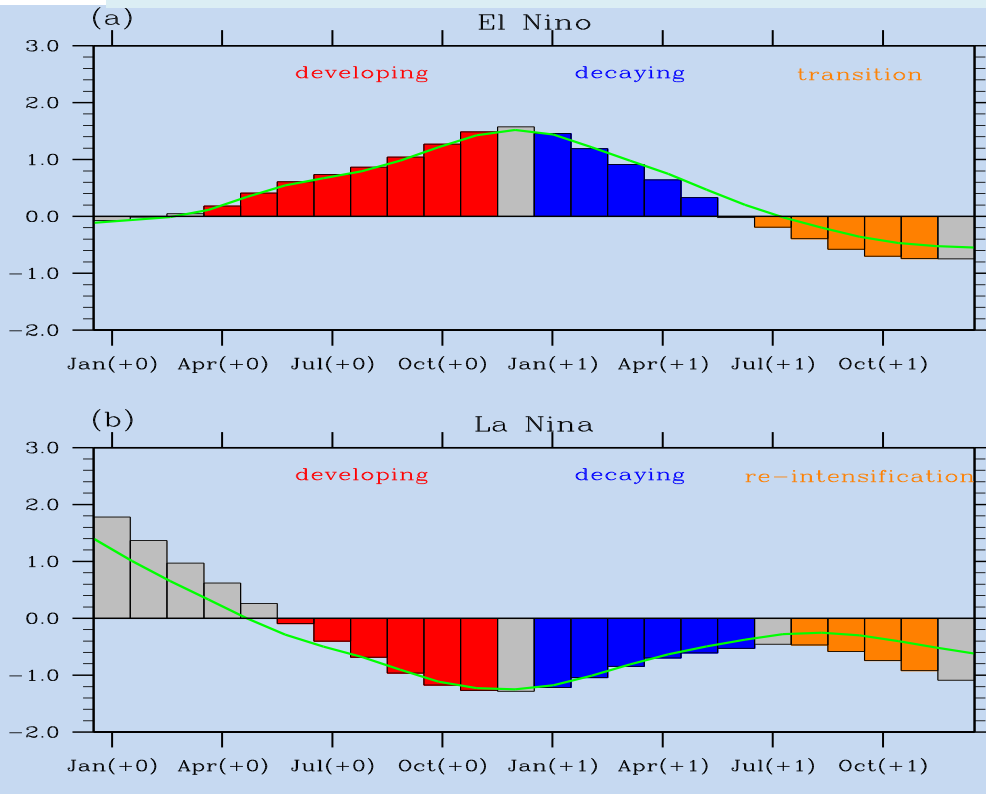
Forcing



850-hPa wind response

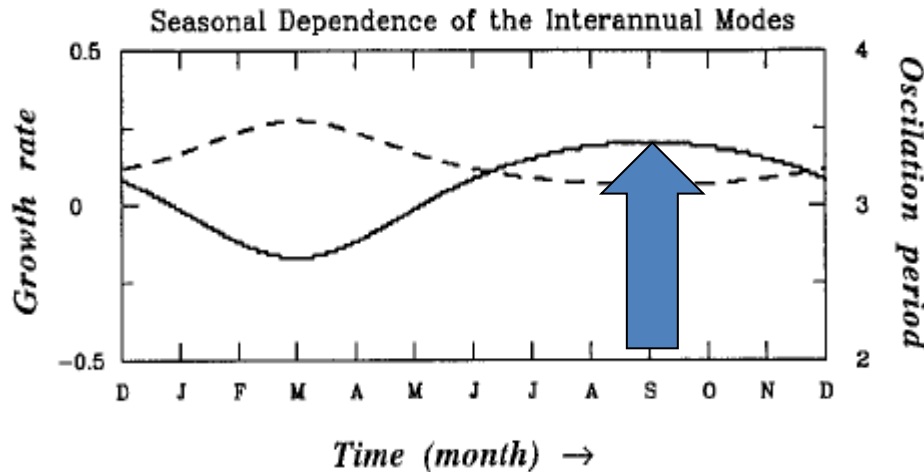


El Nino and La Nina Evolution Asymmetry (cont.)



Key feature: By end of summer of year +1, SSTA has changed its sign for El Nino composite but keep the same sign for La Nina composite.

Why is MLT damping rate during El Nino is 2 times as large as that during La Nina ?



Season-dependent coupled instability (Li 1997, JAS): Both Bjerknes TH feedback and Z. Advective feedback are strongest in northern fall !

$$\frac{\partial T'}{\partial t} \approx -u'T'_x - w'T'_z - \bar{w}T'_z$$

Mixed Layer Heat Budget during El Niño and La Niña decaying phase

	dT'/dt	Adv.	Hflx	Sum	$-u'\partial\bar{T}/\partial x$	sw'	lh'
El Niño	-0.28	-0.12	-0.20	-0.32	-0.19	-0.07	-0.14
La Niña	0.13	0.06	0.11	0.17	0.10	0.04	0.06

Budget analysis domain (180-80W, 5S-5N)

→ Most of previous studies emphasized the **dynamic effect** of wind, here our mixed layer heat budget analysis shows that the **thermodynamic (heat flux) effect** is as important as the dynamic effect (**Chen, Li, et al. 2016, JC**)!

Ocean-Atmosphere Precursor Signals Associated with Super and Regular El Niños

Chen, L., Tim Li, Swadhin K. Behera, Takeshi Doi, 2016: Distinctive precursor air-sea signals between regular and super El Niños. *Adv. Atmos. Sci.*, 33, 996-1004.